Are vegetation index maps derived from sUAS-mounted multi-spectral sensors an accurate predictor of yield in potatoes?

by

Evan MacDonald

A thesis Presented to the University of Prince Edward Island

In fulfillment of the thesis requirement for the degree of

Master of Science in Environmental Science

Charlottetown, Prince Edward Island, Canada 2018

Abstract

Potatoes are an expensive crop to grow, and many inputs such as fertilizers and pesticides are required to ensure that the product is marketable. With advancements in GPS technology over the last three decades, one technology that has come to the forefront in farming is Precision Agriculture (PA). PA assumes that not all parts of a field are uniform, and that by tailoring management decisions to certain areas of a field, farmers can improve production and possibly reduce inputs. Adopting PA in the potato industry makes sense, as there is much to be gained in terms of increasing production as well as mitigating the environmental impacts of industrial farming.

Two tools which fall under the umbrella of PA are the yield monitor and Small unmanned aerial systems (sUAS). sUAS have the ability to collect high resolution remotely sensed data for agriculture. When multi-spectral sensors are mounted to sUAS, algorithms (vegetation indices) can be applied to the data to assess spatial characteristics related to field health. Yield monitors are tools which measure the quantity or quality of production throughout the field. They are synced with GPS systems and can assist a farmer to identify which parts of a field produce higher or lower yields than others. The resultant yield data can be viewed as a report card of a field and used in informing management decisions.

In this study the question was posed: are vegetation index maps derived from sUAS mounted multi-spectral sensors an accurate predictor of yield in potatoes? This study used sUAS to survey a 30 acre potato field in Indian River, PE, Canada four times

throughout the growing season (Once before planting for elevation mapping – May 7th 2016; 39 days after planting – July 13th 2016; 67 days after planting – August 10th 2016; and 98 days after planting – September 10th 2016) . These dates equate to growth stages II, IV and late IV respectively (vegetative growth and tuber bulking) and were chosen at separate growth stages to determine which stage correlated greatest with yield. Growth stage I is considered pre emergence, while growth stage V is considered maturation where photosynthesis decreases and vines die off – these stages were not relevant for capturing imagery. It was expected that the areas of the field that appeared healthiest early in the growing season would produce the greatest yield at harvest. The collected sUAS data were correlated with yield harvest data to examine relationships between in-season field health maps and actual yield in lbs/acre. Correlations between sUAS data collected in July, and yield data collected at harvest, indicate that the farmer can get an idea of which areas of a field will produce the highest yield early in the growing season, and use this data to make informed management decisions on their farm.

sUAS technology is rapidly evolving and adoption of these analytical tools on the farm will be more common as they become more affordable and user friendly. As the large range of sUAS collected data becomes more manageable, farmers and agronomists will be able to apply this technology on their crops and thereby, improve the ways they farm in order to maximize yields and minimize inputs.

Acknowledgements

This study was funded by the University of Prince Edward Island, and the Marine Environmental Observation, Prediction and Response Network (MEOPAR). Field assistance was provided by members of the UPEI Climate Research Lab with special thanks to Andy MacDonald, Andrew Clark and Derek Ellis.

I would like to thank my thesis supervisor Dr. Adam Fenech (University of Prince Edward Island), my committee members – Dr. David Burton (Dalhousie University) and Dr. Michael van den Heuvel (University of Prince Edward Island), external examiner Dr. Anthony Shaw (Brock University), as well as Steve Watts (Genesis Crop Systems Inc.) for their input and assistance with this project. I would also like to thank Oyster Cove Farms in Hamilton, PE for cooperating with me during this project and allowing me to use their field as a study site as well as providing yield data.

I would not have been able to complete this project without the understanding and support from my family and employer. Thank you to my wife Stephanie for encouraging me to pursue my Masters and my daughter Quinn, who was only one week old when I began this project. Thanks to the Prince Edward Island Department of Agriculture and Fisheries, as well as Communities, Land and Environment for allowing me the flexibility to work on my Masters while holding a full time job.

Table of Contents

List of Figures

List of Abbreviations

CORS – Continuously Operating Reference System

DSM – Digital Surface Model

ENDVI – Enhanced Normalized Difference Vegetation Index

ExG – Excess Green

GAI – Green Area Index

GCP – Ground Control Point

GIS – Geographic Information Systems

GNSS – Global Navigation Satellite System

GPS – Global Positioning System

LIPO – Lithium Polymer

MODIS – Moderate Resolution Imaging Spectroradiometer

MTCI – MERIS Terrestrial Chlorophyll Index

N – Nitrogen

NDVI – Normalized Difference Vegetation Index

NGB – Near Infrared, Green, Blue

NIR – Near Infrared

PA – Precision Agriculture

REIP – Red Edge Inflection Point

RGB – Red, Green, Blue

SUAS – Small Unmanned Aerial System

UAV – Unmanned Aerial Vehicle

VEG – Vegetative Index

VI – Vegetation Index

VTOL – Vertical Takeoff and Landing

WDVI – Weighted Difference Vegetation Index

Chapter 1: Introduction and Literature Review

The potato industry on Prince Edward Island is a polarizing one. It generates more than $1 billion for the provincial economy and creates over 8,000 jobs which represent 12.1 percent of total employment on Prince Edward Island (MacDonald, 2012). While being the largest economic driver, the agriculture industry has been blamed when fish kills have occurred due to “highly toxic” pesticides reaching waterways, and there have been many claims that chemicals used in the industry are a contributing factor in the province having some of the highest cancer rates in Canada. (MacDonald, M. 2013; Mittelstaedt, 2006; Canadian, 2013)

Potato production dominates the landscape in P.E.I. with an average of approximately 90,000 acres planted per year and an annual output of 1.3 million tons in 2016, which is the most in Canada (PEI, 2016). Potatoes are an expensive crop to grow, costing over $3,000 per acre (Trainor, 2009). They require costly inputs such as fertilizers, herbicides, and pesticides to be marketable. If not managed prudently, these inputs can put at risk the Island’s environment.

Potato producers now have access to technologies that can benefit them in many ways, such as increasing production and reducing input costs. Global Positioning System (GPS) technology, yield monitoring equipment, soil quality monitoring tools and remotely sensed imagery all have the ability to influence farmers’ management decisions. With potatoes being such a costly crop to grow, farmers can now apply these available tools and data to produce their crops more efficiently and economically.

Technology will be vital in addressing the economic and environmental impacts of agriculture both in Canada and around the world. With global population expected to reach almost 10 billion by 2050, there will be increased pressure to produce more food while striving to be environmentally and economically sustainable (United Nations, 2015).

1.1 Precision Agriculture

Finding a balance between economic gain and environmental sustainability can be a difficult task for farmers. One farming practice that aims to address these issues is Precision Agriculture (PA). PA can be defined as "a management strategy that uses information technology to bring data from multiple sources to bear on decisions associated with crop production" (National Research Council, 1997). "Precision agriculture comprises a set of technologies that combines sensors, information systems, enhanced machinery and informed management to optimize production by accounting for variability and uncertainties within agricultural systems" (Gebbers and Adamchuk, 2010). One way to implement PA is to capture crop growth information in real-time (Zhang et al., 2002). Although information obtained from high-resolution satellite imagery has been used to reach this goal for a long time, the availability, often prohibitive costs, timing, and interpretation of such data limit its applications, which would suggest an alternative way for this application in precision agriculture (Yu et al., 2013). Specifically, images taken by sUAS are shown to be a potential alternative given their low-cost of operation in monitoring, high spatial and temporal resolution, and their high flexibility in image acquisition programming (Zhang and Kovacs, 2012). PA works under the assumption that not all parts of a field are uniform, and it has been practiced commercially since the 1990's with over one third of US mid-western farmers already practicing some form of PA (Mulla, 2013).

PA can be summarized in three steps: 1) Identify where, when, and how much variability is present within a field, 2) Apply agronomic expertise to analyze the within-field variability in order to determine how best to manage it, and 3) Managing the within field variability to enhance productivity while minimizing environmental risks (Cambouris et al, 2014). One of the most efficient methods in identifying variability within a field is through remote sensing.

1.2 Traditional Methods of Collecting Remotely Sensed Data

Traditional platforms for gathering remotely sensed data for PA include satellites, manned aircraft, and handheld sensors. Satellite imagery is steadily improving from 56 x 79m per pixel resolution acquired by Landsat 1 launched in 1972, to 30cm per pixel resolution captured by WorldView satellites today (Mulla, 2013). The two largest limitations for satellite imagery are the presence of cloud cover, and temporal and spatial resolution.

Satellite imagery is often used to predict yield in crops around the world. A study by Ferencz et al in 2004 examined the relationship between a newly developed vegetation index – General Yield Unified Reference Index (GYURI) and yield data in corn fields in Hungary over an eight year span and found that there was a high correlation (R2 = 84.6-87.2). The authors deduced that this robust method would be useful for county, region and country level yield estimation (Ferencz et al, 2004). Considering the average field size in Prince Edward Island - county, region or country level yield estimates would not be useful for a farmer trying to make in season management decisions on their crops. Similarly, a study in France in 2008 by Cunha et al looked at the relationship between NDVI and yield in grapevine crops for the production of wine and found that NDVI was a strong predictor of yield on a regional scale at seventeen months before harvest. Statistical tests indicated that the wine yield forecast model explained 77-88% of the inter-annual variability in wine yield (Cunha et al, 2008). Satellite imagery has proven to be valuable in estimating yield at regional scales, but for a farmer to address individual fields at the management zone level, higher resolution data is required. A study by David M. Johnson in 2016 looked at correlating multiple vegetation indices derived from Moderate Resolution Imaging Spectroradiometer (MODIS) satellite imagery with yield throughout a whole growing season among ten different crops, including potatoes. In reference to potatoes, he found that “NDVI is strongly positively correlated at over 0.9 in early summer and then swings negative at more than −0.7 late in the season.” (Johnson, 2016)

Manned aircraft have been used to capture aerial images of crops as well. A study by R.N. Colwell in 1956 looked at the application of aerial imagery in assessing healthy and diseased wheat crops. The author determined that a photo interpreter could detect healthy wheat, oats and barley and also identify diseases such as black stem rust in wheat and oats. The author also noted that by using only small scale black and white photos, disease could be detected early enough for appropriate treatment. Colour photos would allow the interpreter to estimate disease severity and yield deduction with reasonable accuracy (Colwell, 1956).

Manned aircraft remain more feasible for capturing regional scale imagery rather than field scale analysis. The speeds at which a manned aircraft operate do not allow it to capture as many high resolution photos as a sUAS is able to at the field scale. Purchasing a manned aircraft and obtaining a license to fly and capture aerial imagery is not realistic for a farmer seeking individual field level data. Service providers often have expensive hourly rates. Some companies such as GeoVantage (North Andover, MA, USA) are taking advantage of groups of farmers in a region and capturing imagery over larger areas which enable them to keep costs down.

Handheld optical sensors, such as the Greenseeker (Trimble Navigation Ltd., Sunnyvale, CA, USA), have been used to capture canopy reflectance information in crops as well. Typically used to take measurements at 0.5 – 0.6m above the crop, these sensors can give instant NDVI (Normalized Difference Vegetation Index) readings which indicate chlorophyll levels in the plant (Quebrajo et al, 2015). The challenge with handheld sensors is that it is manually intensive and not realistic to capture measurements across an entire field. Tractors have been outfitted with sensors, which eliminates manual input, but imagery is only captured where the tractor drives -and farmers like to minimize the impact of driving they do in a field in order to reduce soil compaction issues and prevent yield losses.

A relatively new tool for collecting remotely sensed data is the small unmanned aerial system (sUAS), commonly known as a drone. The affordability of these systems, along with their relative ease of use has made them an attractive option for those working in agriculture in the past few years. sUAS have major advantages over traditional methods of gathering remotely sensed data. These systems can be deployed at almost any time (depending on weather and local regulations), and capture high resolution data. Data collected by sUAS used in agriculture are typically ~3cm per pixel, in comparison to current satellite imagery which may be 30cm – 30m per pixel resolution (Digital Globe, n.d.).

Traditional remote sensing platforms have not been widely utilized in the precision agriculture discipline due to several logistical challenges; (1) data acquisition can be costly from these platforms, and (2) they have limited flexibility in terms of temporal and spatial resolution of the data. Fine spatial and high temporal resolution data is required to monitor crops accurately through the growing season for biomass estimation, yield prediction, and early detection of harmful insects and disease. In this regard, advances in sUAS technology and sensor miniaturization can provide great opportunities to tackle the challenges encountered with the traditional remote sensing platforms (Anthony et al., 2014; Bendig et al., 2014; Rey-Carames et al., 2015).

sUAS have the potential to be a superior tool than the previously mentioned methods of gathering remotely sensed imagery in agriculture at the field scale. Outside of the benefits of affordability, freedom of operation, higher spatial and temporal resolution, sUAS can also be used to gather accurate elevation information by leveraging structure from motion (SFM) technology. SfM uses triangulation to recreate scene geometry and builds a 3D model of an object or surface based on multiple overlapping images (Westoby et al, 2012). This is one of the greatest advantages of surveying with sUAS, since highly accurate Digital Elevation Models (DEMs) can be useful in agricultural and environmental applications.

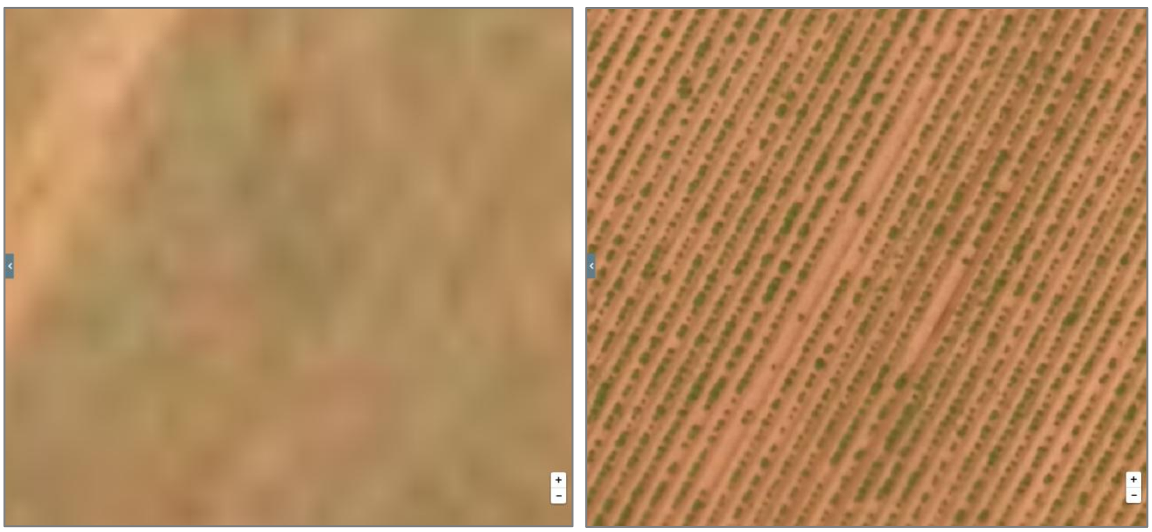

Figure 1: Example of Satellite (left) vs sUAS (right) imagery resolution. Satellite imagery courtesy dronedeploy.com

1.3 SUAS in Agriculture

There are two common types of sUAS: fixed wing, and multi-rotor, which are often referred to as VTOL (vertical take-off and landing). Fixed wing aircraft are generally meant for surveying large areas, and are popular in the Midwestern United States and Canadian Prairie Provinces where fields are typically 160 acres in size or larger. VTOL aircrafts have traditionally been used for close range inspection purposes, or for surveying small areas. LiPO (Lithium Polymer) battery improvements, and advanced lightweight design have led to the creation of VTOL aircraft that are capable of >30 minute flight times, and the ability to survey > 100 acres on a single battery (DJI, n.d.). VTOL aircraft are particularly useful in Prince Edward Island where fields are relatively small. Fixed wing aircraft requires long landing pathways and open areas for safe operation, whereas VTOL aircraft can easily be deployed and safely landed in tight areas near obstacles such as trees or buildings, if required.

sUAS have the potential to transform agriculture. The Association for Unmanned Vehicle Systems International (AUVSI) reported that UAS integration is expected to contribute $82.1 billion to the US economy by 2025, with 100,000 new jobs being created. About 80% of the commercial application of sUAS is expected to be in agriculture (AUVSI, 2013). Adoption of sUAS in PA is in its early stages, but recently released studies have shown that these tools have the ability to be extremely valuable to farmers and agronomists. “Precision Viticulture is experiencing substantial growth thanks to the availability of improved and cost-effective instruments and methodologies for data acquisition and analysis, such as Unmanned Aerial Vehicles (UAVs), that demonstrated to compete with traditional acquisition platforms, such as satellite and aircraft, due to low operational costs, high operational flexibility and high spatial resolution of imagery" (Matese et al, 2015).

Scientific studies, such as the one performed by Zaman-Allah et al. in 2015, used multi-spectral images collected by sUAS to characterize experimental fields for spatial soil-nitrogen variability and derive indices for crop performance under low Nitrogen (N) stress in maize. The sUAS was able to effectively accomplish both tasks (Zaman-Allah et al, 2015). Ground based studies, such as one by Evert et al in 2012, showed that using crop reflectance data could inform side-dress N rates in potatoes without having an impact on yield. "Side-dress applications supply nitrogen directly to crop roots. This minimizes potential for lost fertilizer due to run-off or leaching, while improving fertilizer uptake" (Hiniker, 2015). This particular study did not involve the use of sUAS, but mentions the tool as being viable for addressing crops. It was determined that the methods used in this study resulted in an average savings of 44kg n/ha and that yield was not negatively impacted. In the Netherlands, where this study was conducted, typical application rates are 250 kg N ha – indicating that a savings of almost 20% was possible, that would result in significant savings for a farmer, as well as minimizing the amount of N which enters the ground (Evert et al, 2012). In a study by Aguera et al, that measured N status in sunflowers, it was found that Normalized Difference Vegetation Index (NDVI) readings derived from sUAS collected imagery, and those collected by ground based radiometer, were similar and proved to be good indicators of N in the field (Aguera et al, 2012). NDVI values derived from sUAS collected imagery represent an entire field, not just random sample areas; therefore sUAS have the potential to be a more comprehensive and superior tool.

A study by Bendig et al. in 2014 looked at using crop surface models derived from sUAS imagery to estimate above ground biomass in barley, which is indicative of yield. The high resolution crop surface models correlated well with plant height reference measurements from the field. Both the crop surface models and plant height measurements also correlated well with fresh and dry biomass and the authors determined that this method has potential for future application by farmers. The main limitation noted in this study was the influence of lodging cultivars in later growth stages which produced irregular plant heights (Bendig et al, 2014).

A study by J. Torres-Sanchez et al. in 2014 examined the use of low cost sUAS captured imagery from a visible spectrum camera and vegetation indices derived from that imagery to perform vegetation fraction mapping in wheat. The goals of the study were to determine which indices (out of 6 that were tested) performed best, and to study the influence of flight altitude on classification accuracy. The study concluded that ExG (Excess Green) and VEG (Vegetative Index) indices achieved the greatest accuracy in vegetation mapping while flight altitude (30m vs 60m) had little impact on the accuracy. With the ability to discriminate vegetation early in the growing season, PA applications such as site specific weed management are possible to implement based on sUAS captured imagery. This application is not possible with traditional forms of remotely sensed imagery since spatial resolution is not sufficient (Torres-Sanchez et al, 2014).

sUAS technology adoption does not come without its own set of challenges. Learning to fly sUAS and process data can be challenging enough for a farmer; they then have to adhere to a national set of regulations and legislation that comes along with the threat of fines for non compliance. sUAS specific liability insurance is a requirement in Canada for any individual using these tools for commercial purposes (Transport Canada, 2018). These factors, along with understanding how to manage and manipulate large quantities of data can be a deterrent for farmers looking to adopt sUAS technology. The benefits will have to vastly outweigh the challenges before sUAS become a common tool on the farm.

1.4 sUAS Collected Data and Vegetation Indices

While observing a robot flying around a field can often captivate a farmer or a scientist, it is the data that is most important. Using an autonomous sUAS to collect hundreds of images over a field is often the least challenging aspect of applying this technology in agriculture. Making use of the data, and getting results that will either increase revenues for the farmer and-or improve environmental sustainability (and hopefully both), are the two most important objectives.

One of the most significant determining factors in the quality of data collected by sUAS is the camera. In agriculture, there are many different cameras being used to capture remotely sensed data. These cameras range from basic RGB spectrum (Red, Green, Blue) to multispectral and hyperspectral systems which can cost hundreds of thousands of dollars. For characterizing field health in crops, multispectral cameras are most common today. Multispectral cameras range from consumer-grade, such as the Canon S110 NGB which has a modified filter designed to detect near-infrared light, to more specialized cameras such as the Parrot Sequoia (Parrot SA, Paris, FRA) which captures 4 separate bands of light – green, red, red edge, and near infrared as well as RGB. Capturing more bands of light simultaneously provides a greater opportunity to apply different Vegetation Indices (VIs) and examine plant characteristics (Parrot, 2016).

Hyperspectral sensors such as the AISA-Eagle, which was used in a study by Nigon et al (2015) in detecting N stress in two potato cultivars, capture 63 narrowbands of light covering the visible and near-infrared portions of the spectrum ranging from 401-982 nm. These sensors are typically mounted to manned aircraft or satellites, but are becoming more compact for use with sUAS. sUAS specific hyperspectral sensors such as the Micro-Hyperspec (Headwall Photonics, Fitchburg, MA, USA) cost over $50,000 USD (Micro Hyperspec, 2016). Not long ago, it was either high spectral resolution + low spatial resolution or high spatial resolution + low spectral resolution, but it is becoming more common to see hyper-spectral imaging systems weighing less than 1kg mounted to sUAS and capturing high spatial resolution data (Zhang, 2016). The weight of a camera system (known as payload) on sUAS has a significant impact on battery life. A combination of smaller sensors, along with increased battery life will enable sUAS to cover more ground and make sUAS mounted hyperspectral cameras more usable in agriculture. Hyperspectral sensors have greater abilities in terms of targeting and identifying specific diseases in crops due to the range of bandwidths they can capture, but require more intensive processing strategies (Adao et al, 2017).

Manipulating the imagery captured by sUAS provides a way to gather information which may give indications of biomass, chlorophyll content, nitrogen content or other crop characteristics. “A common and simple way of extracting information about crops from digital images is through the estimation of vegetation indices (VIs)” (Rasmussen et al, 2016). NDVI, developed by NASA in 1979, is the ratio of near infrared (NIR) minus red divided by NIR plus red, and is one of the most common VIs used in agriculture. Other VIs such as REIP (Red Edge Inflection Point), ENDVI (Enhanced Normalized Difference Vegetation Index), WDVI (Weighted Difference Vegetation Index), GAI (Green Area Index), MTCI (MERIS Terrestrial Chlorophyll Index), and others have proven to be valuable in examining potato crop canopy (Nigon et al, 2015; Evert et al, 2012, Geipel et al, 2016). The type of camera being used, and the bands of light it collects, will determine which VIs are possible to implement. Cameras that capture NIR light are commonly used in agriculture because plants reflect more NIR light when they have higher chlorophyll levels and are healthy. When plants are stressed they reflect lower levels of NIR light and this will be apparent in VI maps.

1.5 Data and Image Processing

Before VIs are applied to imagery, the individual pictures are stitched together into an orthomosaic using photogrammetry software such as Pix4D (Pix4D SA, Lausanne, SWI). The quality of the orthomosaic is determined by the camera's specifications, as well as flight conditions, altitude, side-lap and overlap of the imagery and other factors (see figure 7). Attention to detail in preparation for the survey is vital, since results are determined by the quality of the data. "Photogrammetry is the science of making precise measurements from photographs" (Photogrammetry, n.d.). Along with stitching 2D images together to create an orthomosaic which can be measured and manipulated in Geographic Information Systems (GIS) software, Pix4D can also generate a Digital Surface Model (DSM) from the images that can be used to perform elevation analysis. Free software such as Microsoft ICE (Microsoft, Redmond, Washington, USA) can stitch imagery together, but georeferencing that imagery so that it can be integrated with ground based GPS, whether they are handheld or tractor based, is important for PA applications. Today's sUAS systems often involve a camera that is directly integrated with the sUAS autopilot where pictures are "geo-tagged" automatically, or the camera itself has built in GPS for recording positions during the flight. Geo-tagging of photos is important because it references the image to a place on the Earth's surface. Built in geo-tagging abilities are not very accurate for sUAS without built in real time kinematic (RTK) systems, and there is often a need to use ground control points (GCPs) that are referenced in processing software such as Pix4D. A typical sUAS GPS system may be accurate within 1-3m, whereas the accuracy of an RTK system connected to a local reference system or base station is accurate within 1-2cm. A study by Gomez-Candon et al found that "a UAV flying at a range of 30 to 100 m altitude and using a moderate number of GCPs is able to generate ultra-high spatial resolution ortho images with the geo-referencing accuracy required to map small weeds in wheat at a very early phenological stage” (Gomez-Candon et al, 2013). This locational accuracy is important for any PA application, specifically if the aim is to apply variable rate application (VRA) of inputs.

Pix4D is capable of applying the vegetation index to the orthomosaic that can be transferred to GIS software where it is analyzed and compared with other spatial data sets such as soil health characteristics, yield data, input rates, and more. Detailed spatial statistics can be derived and correlations between data sets examined in programs such as ArcGIS (ESRI, San Diego, CA, USA), and this is where PA provides real value to farmers and agronomists.

1.6 Objectives, Overview, and Structure of the Paper

The objective of this study is to examine whether VI maps derived from sUAS collected imagery can be used to predict yield in potatoes. Researching this subject revealed that there were no specific studies that looked at this relationship in potatoes using similar, and cost effective sUAS. Moreover, there exist only a few studies using satellite images (Bala and Islam, 2009).

When this project began in September 2015, the goal was to use a Parrot Sequoia multispectral sensor that was expected to be released in April 2016, a month before data collection would begin. The local dealer was not able to ship the unit until Late July 2016 due to a delay caused by a required “hardware modification”.

Consequently, it was necessary to use an alternative sensor. A Canon S110 NGB (Near Infrared, Green, Blue) camera, which is common for NDVI mapping in Agriculture, was used. Limitations of this camera in comparison with the Parrot Sequoia sensor are discussed later in this paper.

The study site is a 30--acre commercial potato field located in Indian River, P.E.I. The field was surveyed four times in the spring/summer of 2016 – early May (before planting), early July, early August, and early September which correlate to growth stages II and IV (as seen in figures 2 and 3 below). The yield data were collected during harvest in October, 2016.

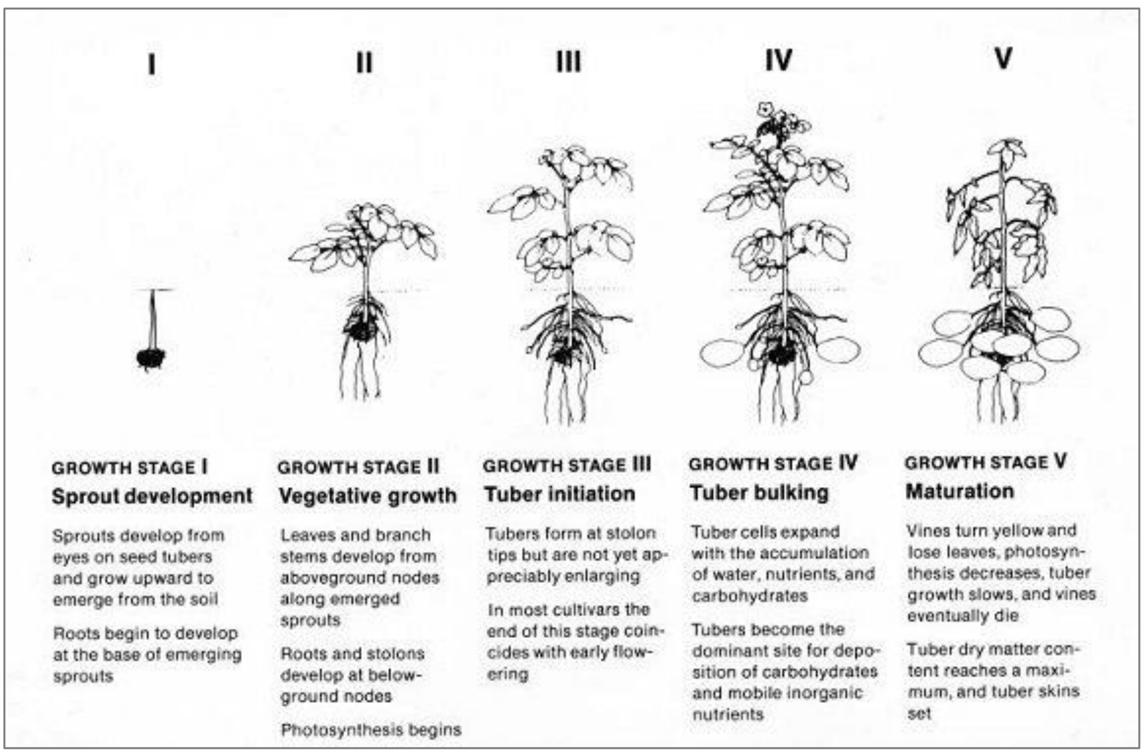

Figure 2: Growth Stages of the Potato. (Johnson, 2008)

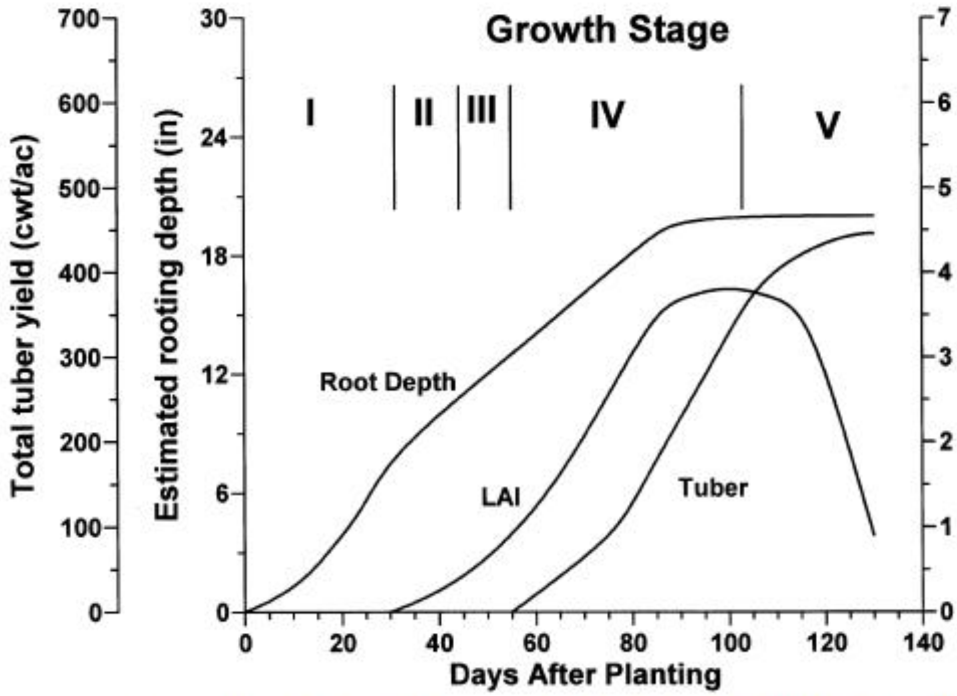

Generalized seasonal progression of rooting depth, leaf area index (LAI), and tuber yield of potato.

Figure 3: Growth Stages of the Potato. Source: Potato Irrigation Management, University of Idaho Extension System

Figures 2 and 3 show the growth stages of the potato. Surveys were performed at 39 days after planting, 67 days after planting and 98 days after planting (Growth stages II, IV, and late IV, respectively). These stages are important to understand because one of the goals in this study is to identify *when* the ideal time is to obtain yield estimates.

Yield is characterized by many factors such as temperature, soil type, moisture levels, PH levels, crop variety, nutrient uptake and more. Due to limited time, resources, and expertise, this study only examined yield as a whole - in correlation with NDVI. Having an understanding of expected yield two or three months before harvest can help farmers in making decisions in terms of nutrient application, irrigation or applying other management practices to their crops depending on which parts of the field are projected to yield higher or lower output than others.

The results from this study, and the investigation into the relationship between NDVI and yield should provide potato farmers with valuable information at a time when sUAS are becoming more affordable and common as agricultural tools. The methodologies, equipment and analysis used in this study can be applied to other crops besides potatoes. A study by Kyle Miller, with AgEagle (AgEagle Aerial Systems Inc., Kansas, USA) looked at the relationship between NDVI and yield in soybeans and found that there was a strong correlation between the two (Miller, 2016). A farmer or agronomist may simply want to understand overall field health, without doing any analysis of the yield. As such, this study could provide some insights to facilitate the analysis of other related problems in PA.

It is expected that the areas of the field that appear healthiest (high NDVI) early in the growing season will be the areas that are most likely to produce the highest yield in terms of lbs/acre.

Chapter 2 examines the methodologies, equipment used, field descriptions, analytical techniques, etc. Pricing for each piece of equipment is noted in order to provide an understanding of the approximate costs of implementing sUAS technology in farm or business operations.

Chapter 3 provides the results of this study along with maps, graphs and tables highlighting the relationships between NDVI and yield. Chapter 4 discusses the results and draws conclusions from the study, as well as addresses any limitations, and provides suggestions to improve methods and analysis going forward. sUAS and camera technology are developing at a rapid pace with engineering and design improvements leading to smaller sizes, longer flying times, better quality imagery and lower costs.

Chapter 2: Methodologies

2.1 Study Site

In order to compare NDVI maps (of potatoes) with Yield maps, an appropriate location was selected based on the following criteria: the farmer/field owner had to have a yield monitor or another method of capturing yield data at harvest at a spatial resolution valuable for understanding relationships, and the farmer/field owner had to be permissive of research involving a sUAS used in that field. A field in Indian River, PE was chosen based on these criteria, and in addition to that, there was other ground-based research being conducted at the site that could be useful in further analysis of this or other studies. (See Figure 4)

The average size of a potato field in Prince Edward Island is about 27 acres, therefore the acreage of the field chosen for this study of 30 acres is close to typical holding throughout the Province (PEI, 2010). The variety of potato was the Russet Burbank.

Figure 4: Study site in Indian River, PE

2.2 sUAS Equipment Used and Flight Planning

The sUAS used in this study was the 3DR IRIS+ (3D Robotics, Berkeley, CA, USA). This sUAS was mounted with a Canon S110 NGB camera, which was modified to "block red light and record near infrared light above 700nm wavelength" (see figure 6) (NDVI, n.d.).

Figure 5: 3DR IRIS+ (left), and Canon S110 Camera (right)

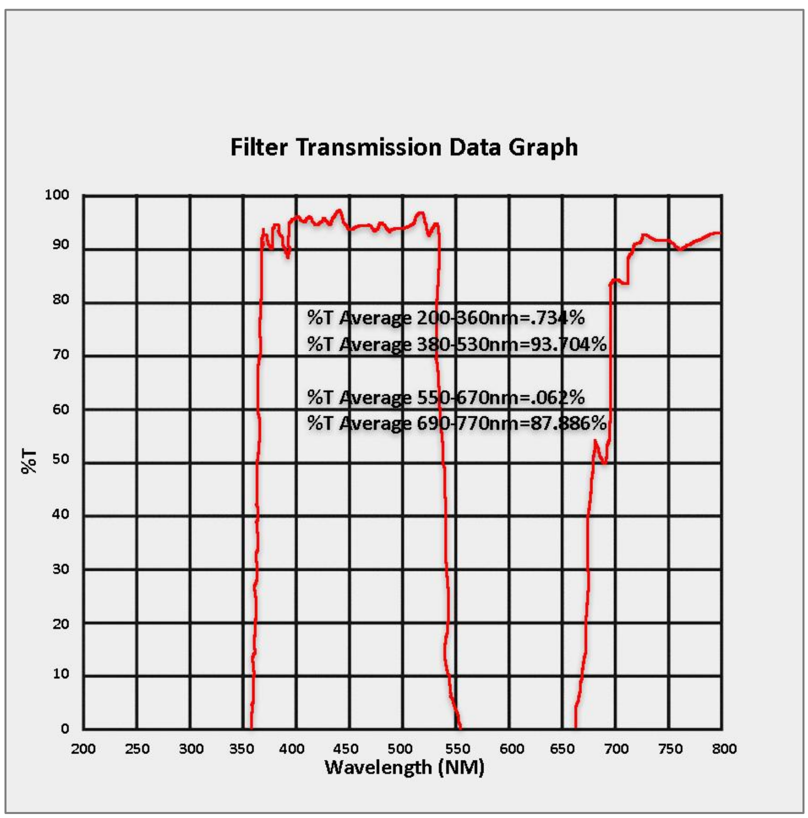

Figure 6: Filter Transmission Data Graph for Canon S110 NGB Camera.
Source: event38.com

The sUAS and camera system were assembled by Event38, located in Akron, OH. The total cost of the system with sUAS, RGB and NGB cameras, extra batteries, and carrying case was approximately $3,000 (USD).

The Canon S110 NGB camera, although commonly used in agriculture, does have its limitations. It is a useful camera to get an overall perspective of field health across a field at one point in time, as long as the user ensures that lighting conditions are optimal. However, it is important to survey the crop only at certain times of the day; between 10am – 2pm is best since the Sun is high and shadows from trees, buildings, etc. are not as long as they are in the early or late hours of the day (DroneDeploy, 2017). Variable cloud poses issues to data collected by this sensor, especially when shadows from clouds can skew the NDVI measurements and healthy plants will appear to have lower readings than expected.

The main benefit of a sensor such as the Parrot Sequoia (the original preferred choice in this study) over the Canon S110 NGB is that the Sequoia is radiometrically calibrated, meaning that it accounts for the amount of incoming incident light radiation by use of an active "sunshine sensor" mounted on the top of the sUAS. This results in more accurate data that are calibrated and absolute, and gives the user the ability to compare datasets over time as well as the flexibility to operate the sUAS in varying light conditions and at different times of the day (Parrot, 2016).

The IRIS+ sUAS has a battery life of approximately 14 minutes (assuming light wind conditions, < 20 km/h). It is good practice to return the sUAS to the ground when battery levels reach 30%. With an expected survey time of 10 minutes, the IRIS+ is capable of surveying ~20 acres when flying at an altitude of 90m and with frontal and side overlap set at 70%. Frontal overlap is determined by how much one image overlaps the next over the track that the sUAS is flying, while side overlap is determined by how much one image overlaps another in a parallel track. This concept can be seen in Figure 7. Ensuring sufficient overlap along track and across track is important, since insufficient overlap can lead to issues with data processing and consequently, result the need to re-fly the mission (Pix4d, n.d.)

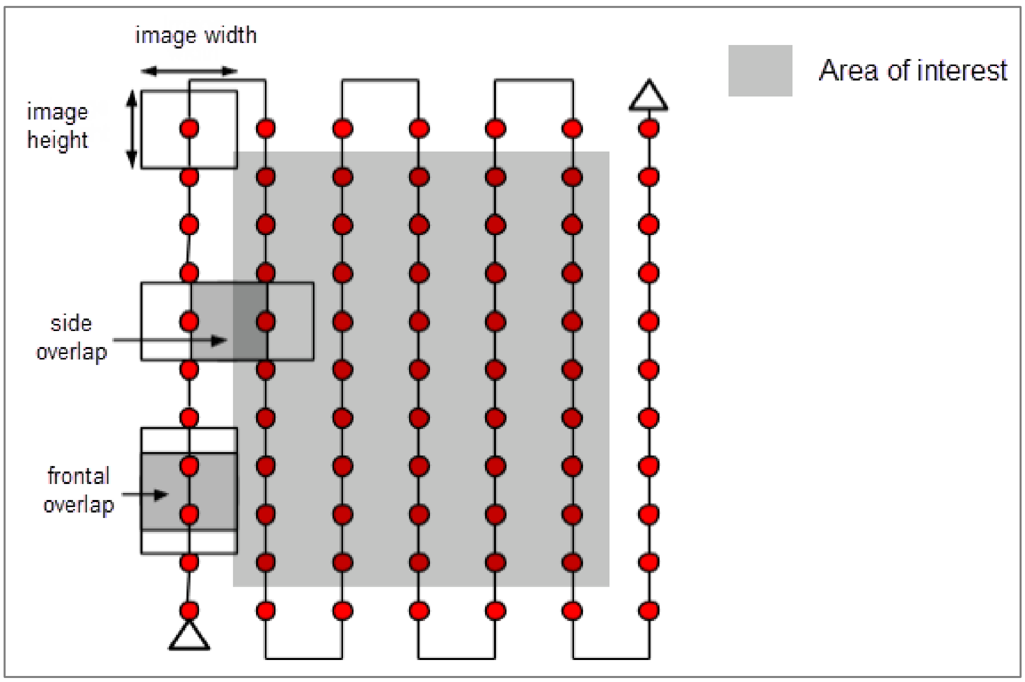

Figure 7: Example of side and frontal overlap in sUAS survey
Source: pix4d.com

The flight control software used in this study was the freely available *Mission Planner* (Michael Oborne). In this software, the user can define an area they would like to survey by drawing a polygon and assigning the camera type, altitude, desired levels of overlap, flight speed, flight orientation and more. Mission Planner connects to the sUAS autopilot via telemetry radio. In this case, a 3DR radio antenna is connected to a laptop running Mission Planner software via USB. The range between the sUAS and laptop running Mission Planner software is 1km unobstructed. Transport Canada's guidelines require the operator to maintain line of sight with the sUAS at all times, which in the case of the 55cm wide IRIS+, is approximately 600-700m. It is important to take this into account when planning a survey - to ensure that the sUAS can reach each end of a field while still remaining in line of sight. It is possible to set up at multiple locations if required for larger areas, but this is inefficient for small fields, and can be prevented with good mission planning.

Missions were planned for the study site in May 2016 and the same plans used for each survey throughout the spring/summer. The field was divided into two surveys since battery life of the IRIS+, and the area to be surveyed, would not permit flying the entire field at once. Images from each survey had to be "geotagged" and combined into one dataset before processing in Pix4D could occur. Geotagging refers to the assigning of a location to each image taken so that they can be referenced to a place on the earth's surface. The camera itself did not have a GPS in this case, but the sUAS did, and the images and flight logs were combined using a geotagging utility developed by Event38. The accuracy of each photo after geotagging is within a few metres, which was sufficient in most cases when viewing relative crop health throughout a field. But in this case where the NDVI maps would be compared with another dataset (yield), it was important that both sets of data were accurately georeferenced. Using ground control points (GCPs) is one method of ensuring accuracy; this concept will be discussed later on in this chapter.

Figure 8: Mission Planner flight control software

Before flying a mission it is important to understand and comply with local regulations regarding the use of sUAS. In this case, since the proposed use was for research, a SFOC (Special Flight Operator Certificate) had to be obtained from Transport Canada. The application process involves highlighting the proposed use of the sUAS, specifications of the sUAS, pilot experience, emergency measures to be taken in the case of an incident and more. The location in this study was a rural area and greater than 9km away from any airport, therefore coordination with NAV Canada and local flight towers was not required.

2.3 Field Data Collection

Before flying the first survey in May 2016, ground control points (GCPs) were placed in four corners of the field. These points consisted of 20” x 20” wooden X’s mounted on 2” x 2” posts which were placed in the ground approximately 18” deep. About 12” of the post was left above ground to ensure that grass would not interfere with the GCPs. In most cases where a location is only flown once, a GCP would be laid upon the ground, measured with a GPS unit, and gathered after the sUAS survey. In this case, where the same field was surveyed 4 times in the year, the GCPs were mounted on posts and only had to be measured once at the beginning of the first survey which saved time in the field.

Figure 9: Image of GCP at one corner of the survey area

The Global Navigation Satellite System (GNSS) system used to record the X,Y and Z positions of each GCP was the Trimble Geo7X. This unit has ~2cm accuracy and costs approximately $20,000. It was connected to a local CORS (Continuously Operating Reference System), Can-Net, and a yearly subscription is paid (~$1,500 per year) to achieve highly accurate spatial data. Each GCP was measured prior to the first survey and inspected throughout the summer to ensure grass did not obstruct the view of the GCP from above. These GCPs would later be referenced in Pix4D software to ensure that the orthomosaic and resultant NDVI map were accurately georeferenced.

Figure 10: Trimble Geo7X Centimetre grade GNSS system
Source: gps-boutique.com

After the mission was properly planned in Mission Planner, the flight could be carried out. The first step is to ensure that the battery is fully charged. This could be checked by inserting the battery in the IRIS, powering it on, and connecting to it through Mission Planner software. Many indicators such as battery life, speed, distance to home, altitude, and more can be viewed in Mission Planner. It is important to keep a close eye on these factors, as the sUAS must be returned to the home point, or at least a safe landing area if issues arise. When it is determined that there is sufficient battery life to carry out the mission, and there are no noticeable physical impediments to the sUAS, then the propellers could be attached. The waypoints were then written to the sUAS autopilot via telemetry radio. Waypoints are created at the initial planning stage and consist of Latitude/Longitude coordinates that the sUAS GPS system must follow. Takeoff consisted of powering up the motors and switching the mode to “AUTO” on the transmitter. The IRIS+ would rise straight up to 60m before heading to its first waypoint. It is important to set the takeoff altitude that the sUAS reaches before heading to the first waypoint to a safe height above any obstacles that may be in the area. The IRIS+ then proceeded to rise to the survey altitude of 90m on its way to waypoint 1.

An altitude of 90m was chosen for this study because it is as high as Transport Canada would allow under the SFOC. Flying higher sacrifices image resolution, but results in a more efficient flight plan due to a wider field of view at higher altitude; thus allowing for less side-lap between images. This uses less battery, along with providing more “keypoints” in the images which improves the quality of the stitched orthomosaic. A flight at 90m over a small field may result in an image containing a hedgerow, road or other feature not seen in an image captured from 60m. These other features are useful in photogrammetric processing software such as Pix4D because the software has a more difficult time stitching homogenous imagery together due to the lack of recognizable differences between images. The resultant resolution of the imagery in this study when captured at 90m was approximately 3.2cm per pixel.

The image capturing process is automated, and begins when the sUAS arrives at its first waypoint. The Canon S110 camera used in this study has what is known as CHDK (Canon Hacker's Development Kit) installed on the SD card. This allows the camera to take pictures at set time intervals determined by the desired frontal overlap which was set when planning the survey in Mission Planner. In this case a photo was taken about every 4 seconds and the IRIS+ flew at a speed of 6 m/s, resulting in one image being captured every 24m.

When the final waypoint was reached, the IRIS+ flew back to the home position and landed automatically. The operator can shift the IRIS+ forward, backward, or side to side if necessary, but it is always recommended to ensure that the sUAS has a safe takeoff and landing area which is level and free from obstructions.

2.4 Data Processing

Before the data could be processed in Pix4D, all of the images had to be geotagged. Event38 has a freely available geotagging utility that matches up the flight log from the IRIS+, with the images saved to the SD card. This provides each image with X, Y and Z coordinates, as well as information in regards to the yaw, pitch and roll of the aircraft. Since it took two flights to capture data across the field, two datasets had to be geotagged separately and then combined into one folder.

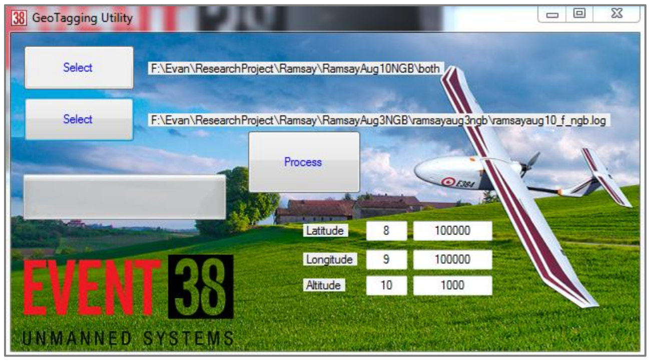

Figure 11: Event38 GeoTagging utility

After a project was started in Pix4D, the 235 geotagged images could then be processed. The first dataset from May 7, 2016 was processed with the goal of achieving an accurate Digital Surface Model (DSM) of the field before planting. The following datasets (July 13, 2016, August 10, 2016, and September 10, 2016) were field health related, and required different processing settings. The desired outputs were selected before processing, and the next step was to use the “GCP/MTP Manager” to mark the images where a GCP was located. After all of the GCPs had sufficient marks (between 3 and 8 is recommended by Pix4D), processing could begin.

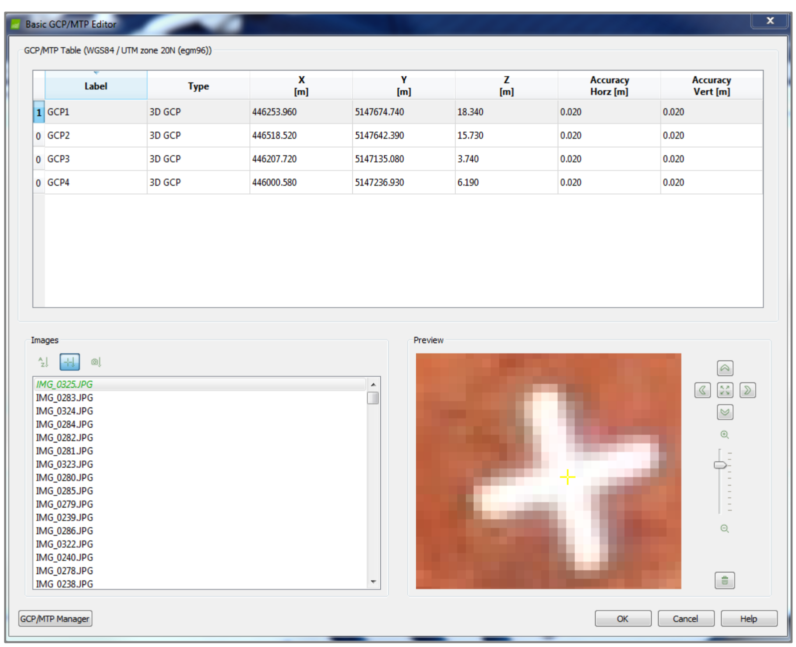

Figure 12: Pix4D GCP Manager

Pix4D produces a quality report for every job that is processed. This report contains details about processing time, georeferencing accuracy, image calibration and much more. The initial processing time for the near infrared (NIR) datasets was approximately 30 minutes. Processing time is greatly determined by the specifications of the PC that runs the software. In this study, the hardware as seen in figure 13 was used.

Hardware	CPU: Intel(R) Core(TM) i7-3770K CPU @ 3.50GHz RAM: 32GB GPU: NVIDIA GeForce GTX 680 (Driver: 9.18.13.1106), RDPDD Chained DD (Driver: unknown), RDP Encoder Mirror Driver (Driver: unknown), RDP Reflector Display Driver (Driver: unknown)
Operating System	Windows 7 Professional, 64-bit

Figure 13: PC Hardware Specs

In processing the NIR datasets, the normalized difference vegetation index (NDVI) was chosen. NDVI is commonly used as a VI in agriculture. "This index is often referred to as a measure of biomass, chlorophyll content, nitrogen content or something else entirely, but it is primarily an indicator that correlates with biomass and other vegetation parameters" (Rasmussen et al, 2016). The typical NDVI formula is the ratio of NIR – Red / NIR + Red (Rasmussen, et al 2016). In this study, since the camera did not record red light, a variation of NDVI, BNDVI (Blue Normalized Difference Vegetation Index) was used. This formula is the ratio of NIR – Blue / NIR + Blue. The camera filter used in this study blocks out red light (see Figure 6), which can be preferable since it prevents any leakage of NIR light in the red band from being picked up. A study by Yang et al examined correlation between BNDVI (from satellite imagery) and yield in cotton and found that it worked similarly and even better in some cases than NDVI (Yang et al, 2006).

After the Index file was created in Pix4D, it was opened in ArcGIS (ESRI, Redlands, CA, USA), where it was then clipped to crop boundaries and analyzed further.

All datasets, including the DSM were clipped to the field edge. The same boundary was used to clip the yield data, and this ensured that both variables in this study (NDVI and Yield) had similar extents. Along with clipping the data to the crop edge, the NDVI datasets were also clipped to only represent the consistent cropping area – meaning areas such as laneways, test strips with rye interseeding, and a section of the field which was planted later than the rest were not included in the analysis (see Figure 14).

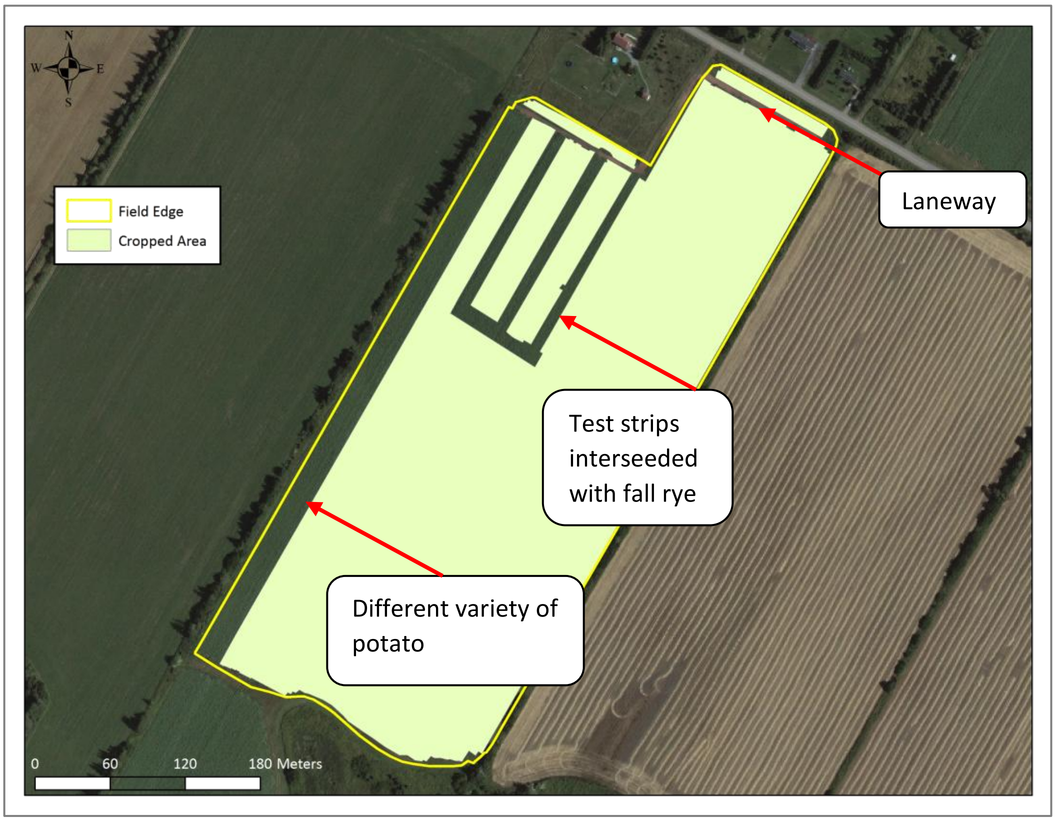

Figure 14: Map showing field edge and cropped area boundaries used for clipping data

After clipping, the NDVI data was classified into 5 classes using the quantiles classification method. Quantiles is a classification method that creates classes with an equal number of features and is useful for showing relative rankings, which is what was desired in this case. Natural Breaks (also known as Jenks) is a classification method that creates classes based on "natural groupings inherent in the data" (ESRI, n.d.). This method failed to show much variation, and NDVI differences were difficult to discern when viewing the whole field on a map.

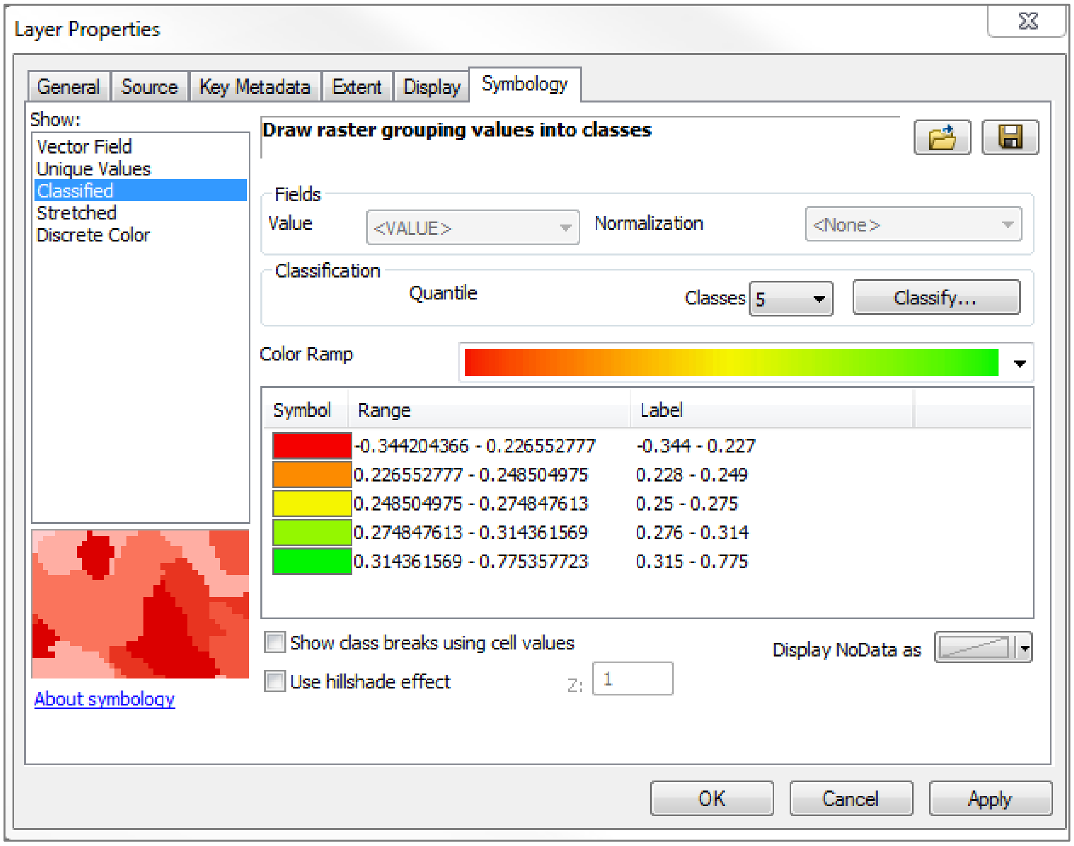

Figure 15: ArcGIS Classification settings

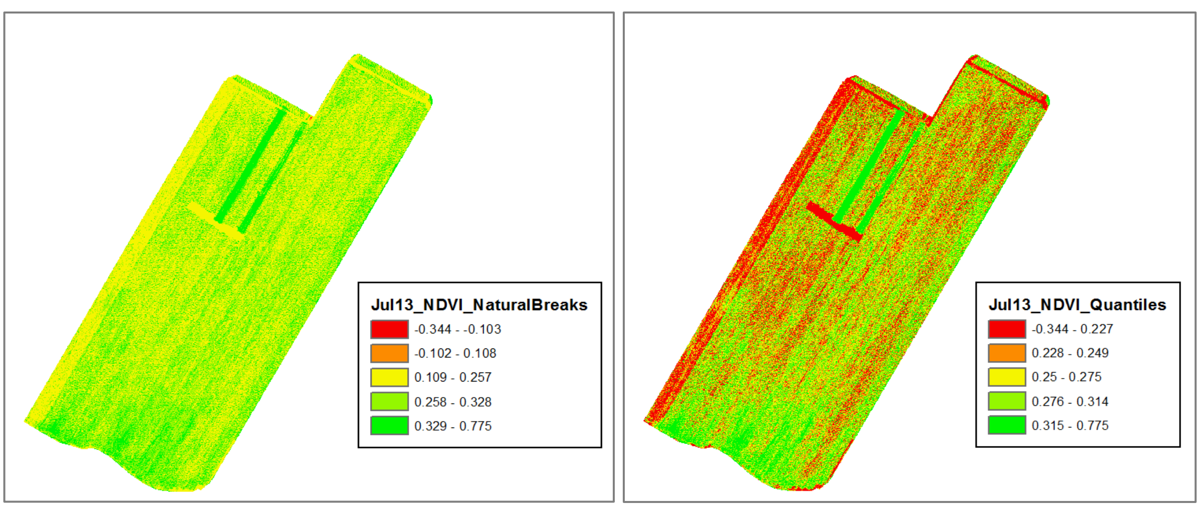

Figure 16: Natural Breaks vs Quantiles Classification

2.5 Yield data

"If you can't measure it, you can't manage it" is a commonly used phrase when it comes to PA. Measuring yield is one of the single most important PA practices a farmer can implement on their farm. The farmer can collect and manage many types of data, whether it is soil sampling, crop health measurements, moisture level monitoring, etc., but if they are not correlating those data sets with yield at harvest then they will not understand how their practices are affecting rates of yield.

Yield data was collected during harvest on October 20th, 2016. The yield monitor used in this study was a Greentronics (Greentronics, Elmira, ON, CA) model. Oyster Cove Farms, the potato producers involved in this project, purchased this yield monitoring system in 2015 and had success in tracking yield for a number of their fields in that growing season. The system consists of a controller, an interface box, two load cells, and a speed sensor. In order to calculate yield, the weight of the crop is measured as it passes over sensors in the conveyor belt of the harvester as the potatoes are being loaded onto the truck, which transports them away for grading, storage and processing. Yield data is then combined with GPS data from the tractor's RTK GNSS system to create a yield map (Greentronics, 2017).

Figure 17: Greentronics yield monitor controller and interface in the tractor

Figure 18: Greentronics yield monitor load cells and speed monitor on the harvester

Monitoring yield is more common in crops such as grain, and measuring it in potatoes presents some challenges. Calibrating the system is vital in order to get quality data. Even proper calibration will not prevent operator error from effecting yield results. During grain harvest, the combine will off load to the truck at either end of the field in most cases, which does not have an effect on the data. In potatoes, the harvester must come to a stop when the truck is full. If the operator of the tractor and harvester shuts off the belt too late when there are no potatoes on it, this can skew the yield data. Likewise, if the operator starts the belt when it is fully loaded and backed up with potatoes, the data may show that there was a greater yield in an area than what was there.

These issues need to be taken into consideration when viewing yield data. In this case, filtering of the yield data was performed in GIS software, ArcGIS. The output file from the monitoring system was a shapefile with over 18,000 data points. These points followed the track of the harvester as it collected the potatoes throughout the field. Twelve rows of potatoes were windrowed into a strip that was picked up by the harvester. This particular farm used 34” rows (multiplied by 12 equals 34 feet wide). The 34 foot value is known as the “swath width” and was accounted for in the data. If this value is not correct then yield values will be skewed.

These data points had many attributes associated with them such as the speed of the tractor, GPS precision, elevation, time, and more. The main attribute of concern in this case was “Dry_Yield”. This measured the amount of potatoes harvested in lbs/acre.

In order to filter the yield data, a histogram was viewed and used to identify anomalies in the data. The bottom five classes of the histogram (seen in figure 19) were eliminated from the dataset. The remaining bottom 2.5%, as well as the top 2.5% (95% distribution remained) were clipped out which resulted in approximately 17,000 values that ranged between 17,098 and 40,072 lbs/acre. When viewed on a map it was clear that the filtered data had eliminated most of the anomalies that were due to operator error in the field. The filtered values were discussed with the farmer who verified that the filtered dataset was much more accurate than the original one that came straight from the yield monitor. Errors in yield data can be expected in most cases during potato harvest since the operator of the harvester is generally more concerned with other parts of the process, such as ensuring the potato truck is not overflowing and that the harvester and tractor are working properly and less concern paid to the yield data.

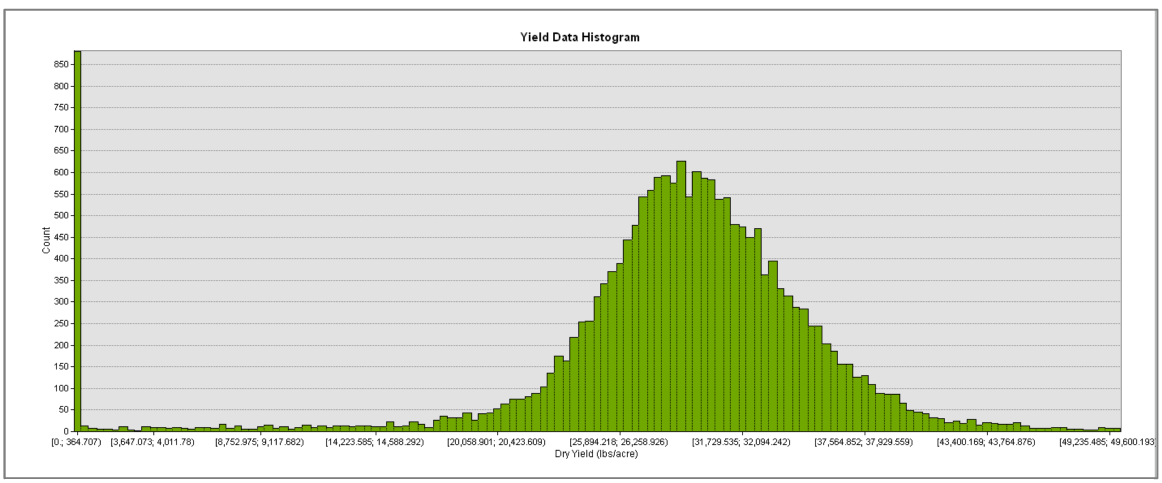

Figure 19: Raw Yield data histogram before filtering

After the points dataset was filtered and anomalies eliminated, it had to be interpolated throughout the field. The other variable in this project, NDVI, was in raster format, which meant that it was a continuous range of 3cm x 3cm squares across the field, each representing a NDVI value. In order to do a proper correlation, each data set had to be in the same format.

The yield data points were interpolated using the “kriging” tool in ArcGIS, available through the spatial analyst extension. Kriging is a geostatistical interpolation method which examines surrounding measured values to derive a prediction for an unmeasured location. “Kriging is a multistep process; it includes exploratory statistical analysis of the data, variogram modeling, creating the surface, and (optionally) exploring a variance surface. Kriging is most appropriate when you know there is a spatially correlated distance or directional bias in the data. It is often used in soil science and geology” (ESRI, n.d.). “Kriging is the geostatistical method of prediction. It is a best linear unbiased predictor on punctual or block supports; best in the sense that its prediction error variances are minimized. It is in practice a weighted moving average in which the weights depend on the variogram and the configuration of the sample points within the neighbourhood of its targets” (Oliver and Webster, 2015).

2.6 Analysis

With yield and NDVI data both in the same format, comparison analysis was then performed. For this project, two methods were used to analyze relationships between NDVI and yield. The first was a "binning" analysis, which grouped the NDVI values into 5 classes based on the Quantiles classification method. The second method was a pixel by pixel analysis of NDVI and yield data at two spatial resolutions: 2m and 6.5m. The third method was a multivariate analysis which included NDVI, elevation, and fertilizer treatment regime to see how these three variables correlated with yield.

The binning analysis began with reclassifying the NDVI data into five classes using Quantiles. The "Raster to polygon" tool within ArcGIS was then used to convert each class to a polygon feature that could be measured. Acreage for each of the five classes was calculated and ranged from 5 -7 acres per class. The "Zonal Statistics as Table" tool was then used with the NDVI zones as the "feature" and Yield dataset as the raster to extract values from. This tool calculated values such as MIN, MAX, and MEAN yield for each of the five NDVI classes. The resulting table was opened in Excel where graphs were created to inspect relationships between NDVI and yield. This process was performed for all three datasets from July, August and September. Potato yield between the NDVI bins was examined using ANOVA followed by a Tukey's post-hoc test.

The pixel by pixel analysis began with "resampling" the NDVI data to match the resolution of the yield data set. Yield data had a resolution of 2m, while the resolution of the NDVI data was much finer at 3cm. There are four main resampling techniques within ArcGIS: Nearest, Majority, Bilinear and Cubic. Each method consists of interpolating values within a desired output cell size (in this case 2m). These methods produced non-satisfactory results, and appeared to skew the NDVI data by creating uncharacteristic linear features along the 2m x 2m grid (see figure 20).

Another method of re-sampling - “Aggregate”, is a tool available in ArcGIS which multiples the cell size by a whole number (60 in this case to achieve a 2m x 2m pixel). This method averages all 60 cells within the desired 2m x 2m cell to create a value. This result was much more appropriate as it did not display any uncharacteristic linear features.

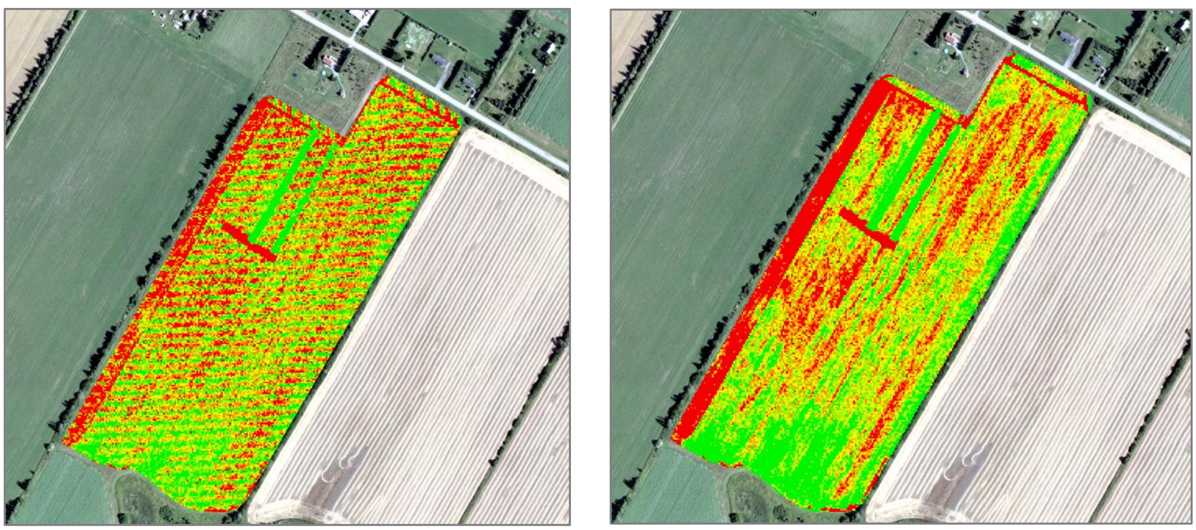

Figure 20: Bilinear Interpolation (left) vs Aggregated resampling method (right)

The “Raster to Point” tool was then used to convert both NDVI and Yield datasets into individual points with single values. After the datasets were in points, the “Spatial Join” tool was used to combine both into one table of approximately 30,000 points, each with a value for Yield and NDVI. The same methods were used to resample the data down to 6.5m resolution, which resulted in approximately 3,000 points. The use of lower resolution data was incorporated to determine whether limiting variability (due to averaging of data across more pixels) would have an effect on the relationship with yield.

Scatter plots and regression analyses were performed on the resultant tables. R-Sq values, which measure how close data are fitted to a regression line and are defined as "the percentage of the response variable variation that is explained by a linear model", were determined (Frost, 2013).

The multivariate analysis included two other variables (besides NDVI) that were examined to determine their relationship with yield: elevation, and fertilizer treatment regime. The Digital Surface Model (DSM), collected in May before planting, was re-sampled from the original 3cm resolution to 2m and 6.5m for analysis with yield and the other variables on a pixel by pixel basis. The study field had two separate fertilizer regimes applied in the 2016 growing season. One was grower standard practice (180 lbs of Nitrogen (N) per acre), which was applied to approximately 2/3 of the field (twenty acres). The other regime was part of the 4R nutrient stewardship program, representing the "Right source at the right rate, right time and right place ®" that aims to "increase production/profitability for farmers while ensuring the future of the agricultural industry" (Fertilizer Canada, 2017). This regime involved application of 60 lbs of N per acre before planting, 80 lbs per acre at planting, and 3 additional applications of 15 lbs per acre in season for a total of 185 lbs per acre. The nine acre area under the 4R program was represented on a pixel by pixel basis with a grid code of "0" assigned if the particular pixel did not have 4R treatment, or "1" if the particular pixel did have 4R treatment. The following map (Figure 21) shows the area for each treatment.

All statistics were performed using statistical software Statistica v13.3 (Dell, TX, USA) at an alpha value of 0.05 to examine relationships between variables.

Figure 21: Fertilizer treatment regime areas

Chapter 3: Results

3.1 Viewing the data

In addition to graphs, the study used maps to display data from this project since all collected information has spatial attributes. Maps provide a way of visualizing data not possible in a spreadsheet, and are very important in PA to identify spatial patterns and trends in agricultural data. Agriculture can be improved through the implementation of GIS as a way to eliminate some of the guesswork involved in crop management, and to record farm specific spatial information year after year.

3.2 Elevation Data

The following map (Figure 22) was created from data collected during the May 7, 2016 flight. The field was in bare soil at this time, and sUAS imagery was able to accurately capture elevation information through photogrammetric processing software Pix4D, along with the use of GCPs.

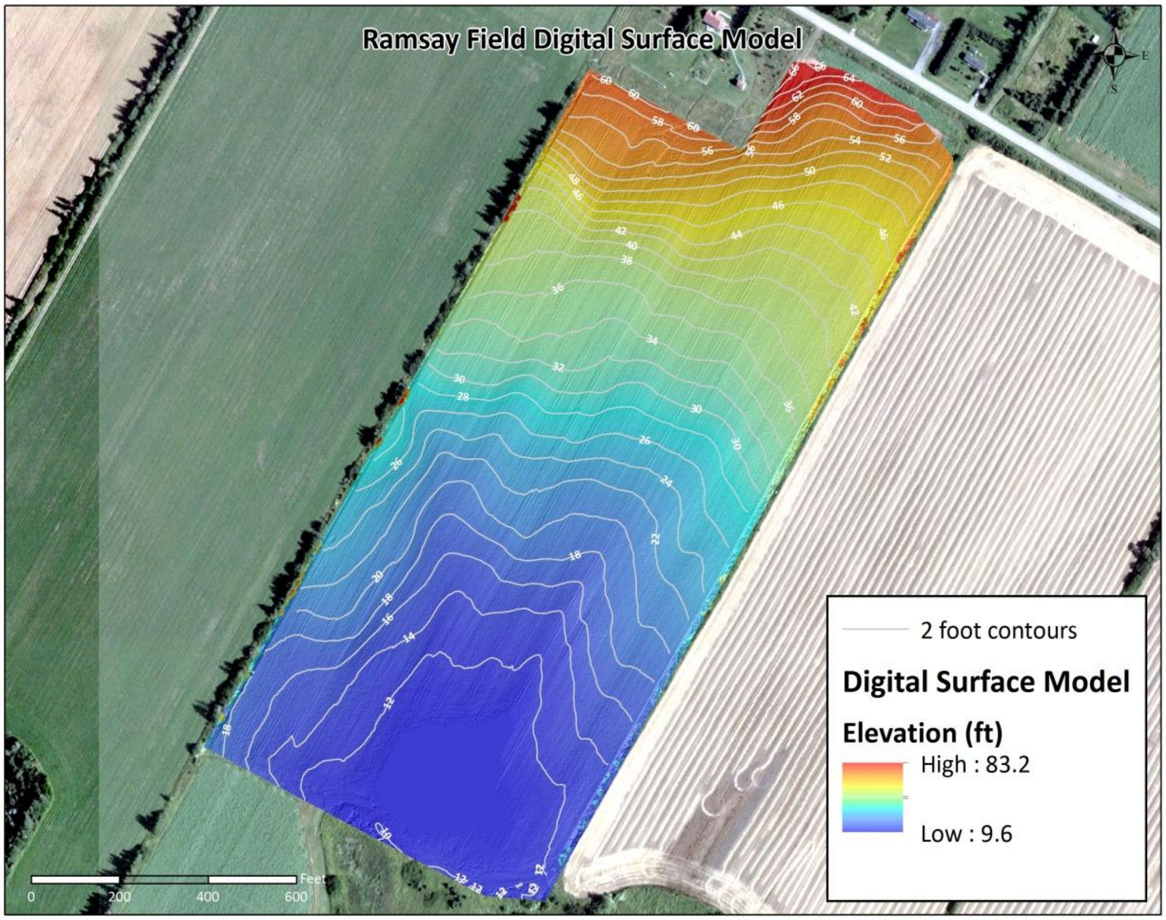

Figure 22: Digital Surface Model of Ramsay Field

This Digital Surface Model (DSM) shows that the field goes from 66 feet above sea level in the northern corner, down to 12 feet above sea level in the southern corner. Rain water and spring melt would drain down to the lower southern section of the field. The contours clearly show a flat area at the southern portion of the field.

3.3 NDVI Maps

The following maps from July, August and September show NDVI values (Aggregated to 2m resolution), clipped to crop area and classified in 5 classes using Quantiles method. For original NIR maps with 3cm resolution see Appendix.

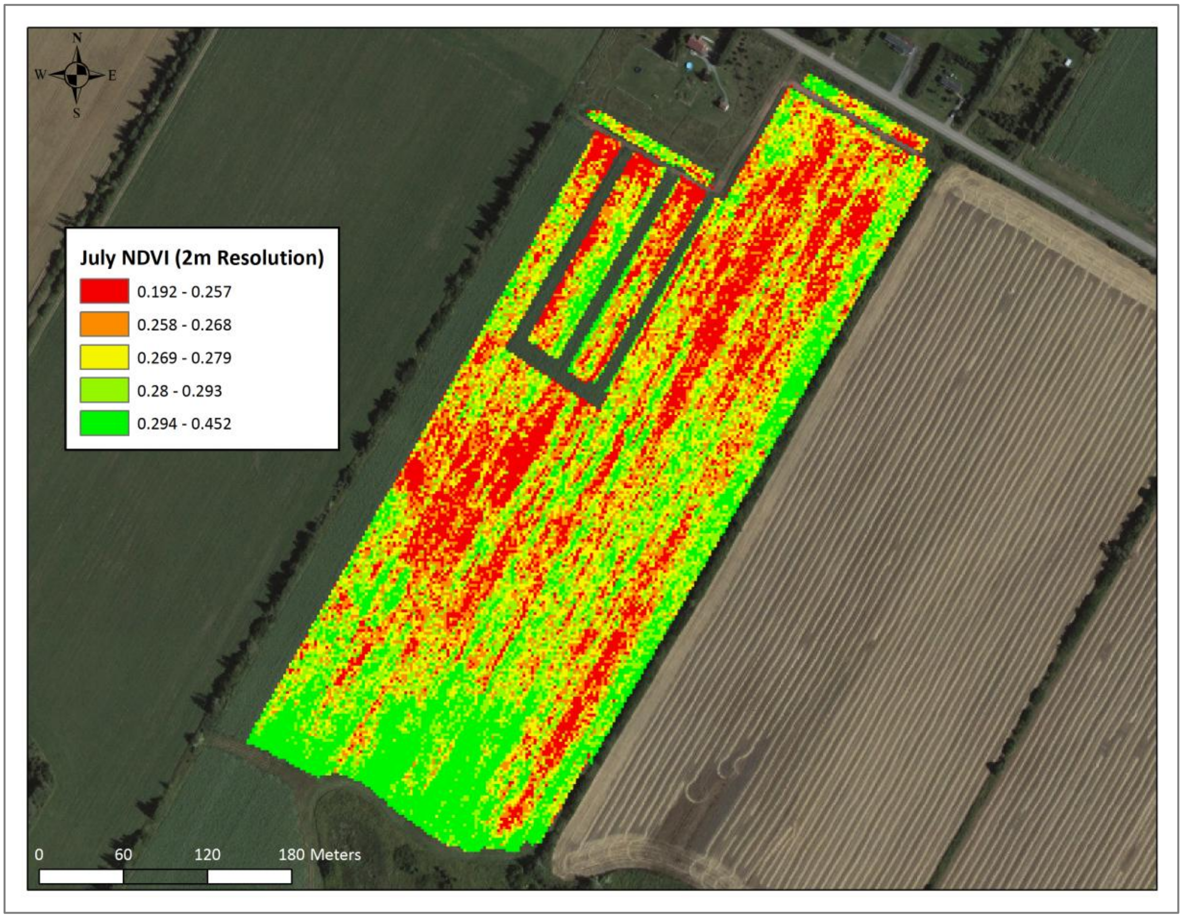

Figure 23: NDVI Map from July

In the July NDVI dataset (Figure 23), the highest NDVI values can be seen in the lower southern area of the field along with a narrow strip on the Eastern boundary.

Figure24: NDVI Map from August

In the August dataset (Figure 24), highest NDVI values can be seen along the Eastern side of the field, as well as the lower southern portion. Lowest values can be seen along the Western side of the field and in the small strips located south of the residential property.

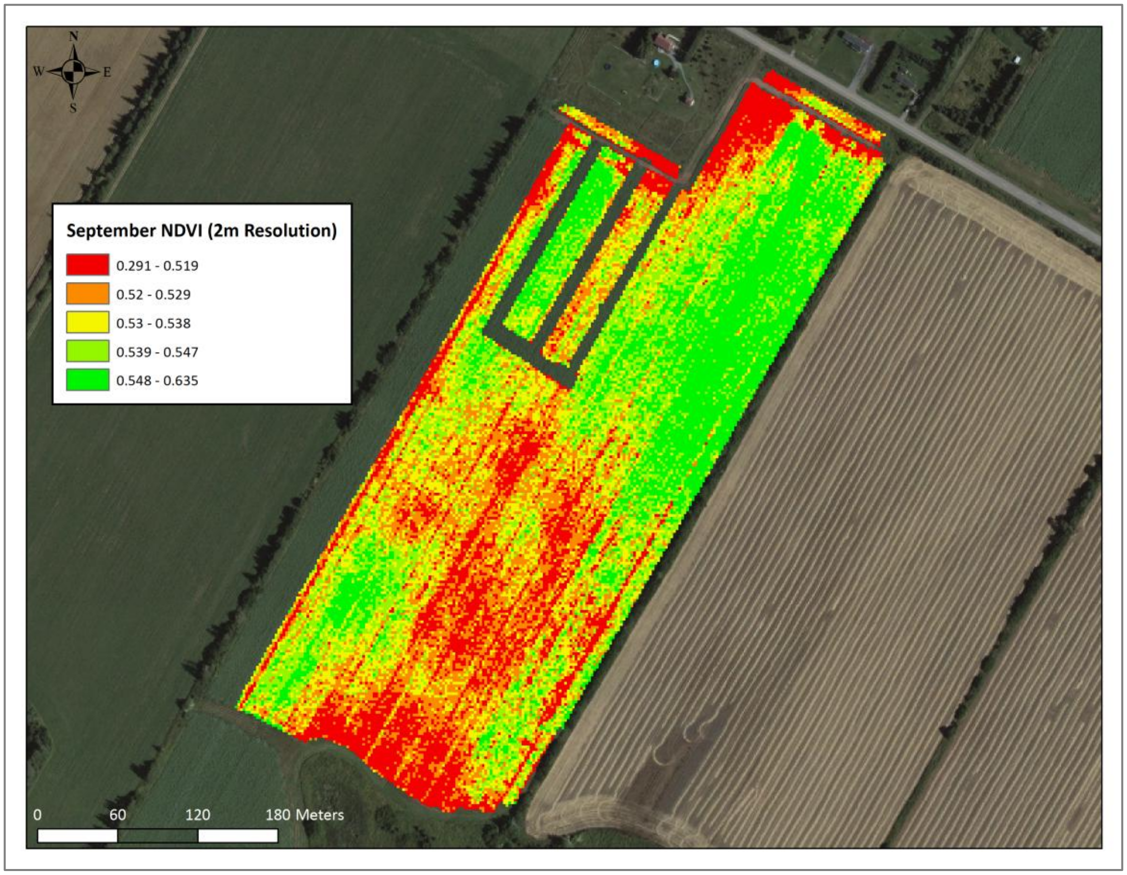

Figure 21: NDVI Map from September

The September dataset (Figure 25) shows highest NDVI values in the North-Eastern section of the field as well as a strip along the Western side of the field. Lowest values can be seen in the low, Southern portion of the field and in the areas surrounding the residential property.

3.4 Yield Data

The following maps show yield data as points (filtered), and as an interpolated continuous surface.

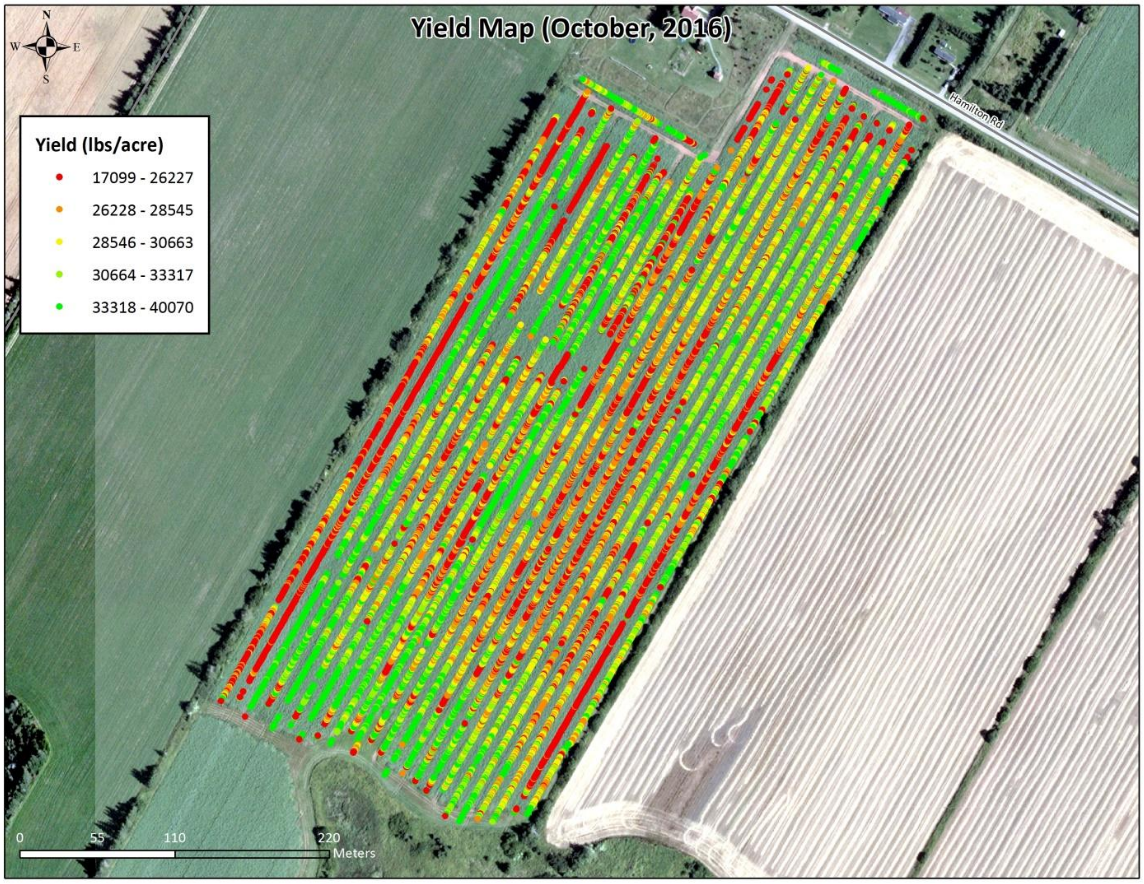

Figure 26: Yield Map after filtering and before interpolation

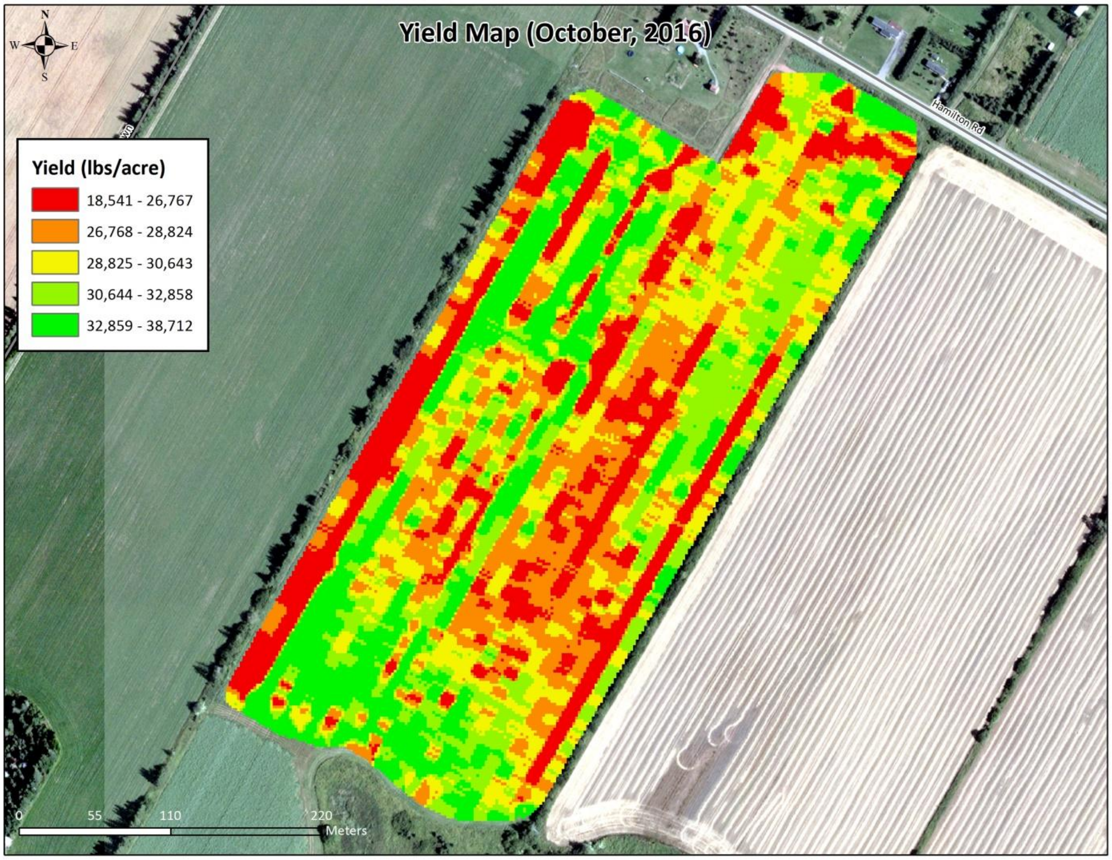

Figure 27: Yield Map after interpolation

The interpolated yield map shows highest values in the lower Southern portion of the field. Lowest values can be seen in the center of the field and along the Western field boundary (this was a different variety of potato), as well as a narrow strip near the Eastern field boundary.

3.5 Binning Analysis Results

The following graphs and charts show the results of the binning analysis.

NDVI and Yield Correlation for July 13th, 2016 Dataset				
NDVI Class	Area (acres)	Mean Yield (lbs per acre)	Min Yield (lbs per acre)	Max Yield (lbs per acre)
1) 0.192 - 0.257	5.6	29853.8	19071.6	38503.0
2) 0.257 - 0.268	5.7	29887.5	18831.3	38298.7
3) 0.268 - 0.279	5.6	29984.5	19246.6	38698.6
4) 0.279 - 0.293	5.7	30215.0	19073.6	38711.7
5) 0.293 - 0.452	5.6	31010.9	20732.7	38711.8

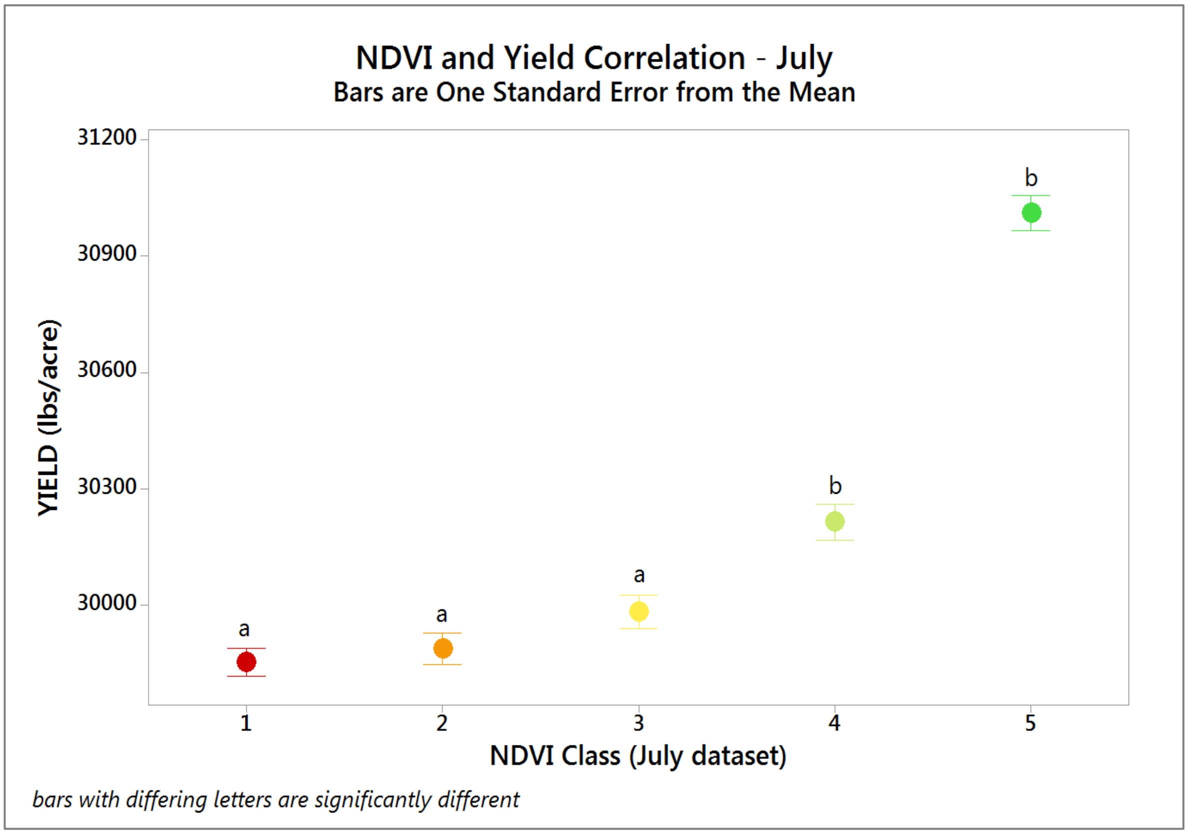

Figure 28: NDVI and Yield Correlation for July

Binning analysis from July shows a good correlation between NDVI and yield. As NDVI values increase so too does yield. The difference between the mean yield for the highest and lowest NDVI class is approximately 1,160 lbs/acre.

NDVI and Yield Correlation for August 10th, 2016 Dataset				
NDVI	Area (acres)	Mean Yield (lbs per acre)	Min Yield (lbs per acre)	Max Yield (lbs per acre)
1) -0.114 - 0.443	5.5	29774.3	18831.3	38698.4
2) 0.443 - 0.465	5.3	29993.0	19002.1	38711.8
3) 0.465 - 0.484	6.0	30220.9	19246.6	38698.6
4) 0.484 - 0.507	6.1	30407.6	18964.2	38559.7
5) 0.507 - 0.852	5.4	30530.9	20634.4	38447.8

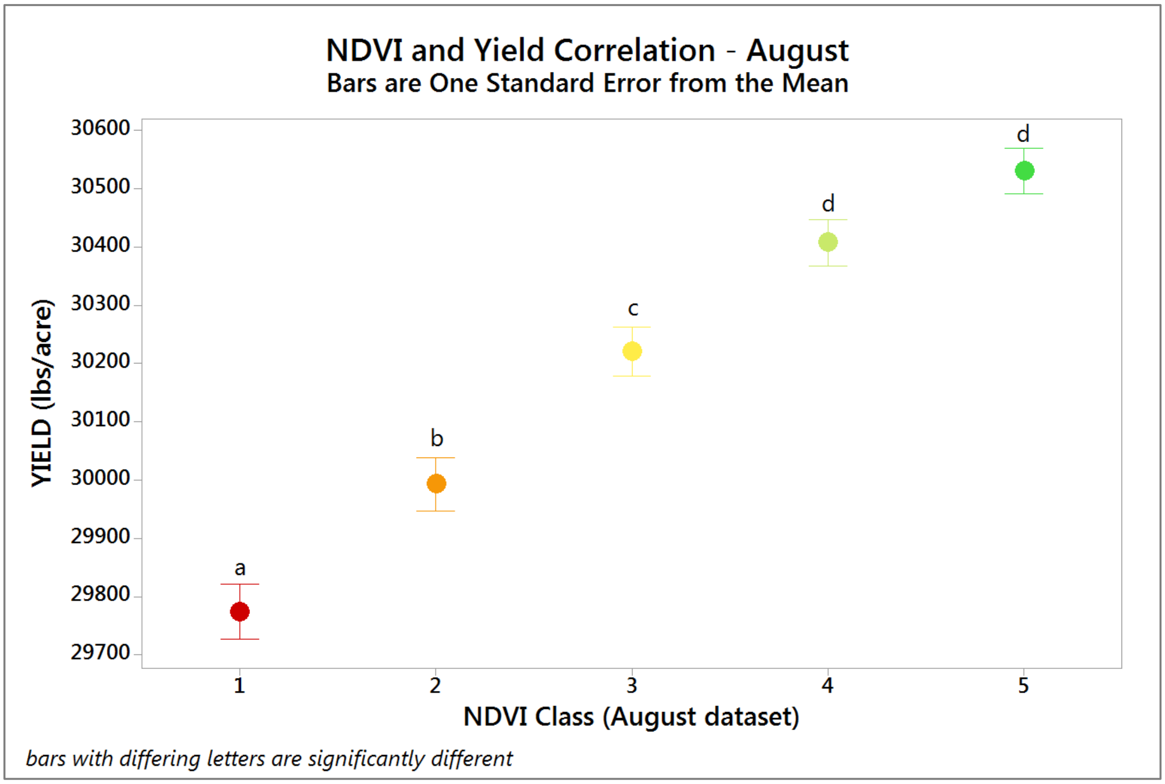

Figure 29: NDVI and Yield correlation for August

Binning analysis for August also shows a good correlation between NDVI and Yield. As NDVI values increase so too does yield. The difference between the mean yield for the highest and lowest NDVI class is approximately 750 lbs/acre.

NDVI and Yield Correlation for September 10th, 2016 Dataset				
NDVI	Area (acres)	Mean Yield (lbs per acre)	Min Yield (lbs per acre)	Max Yield (lbs per acre)
1) 0.291 - 0.519	4.9	29990.1	19248.3	38710.7
2) 0.519 - 0.529	6.1	30030.6	19558.7	38711.8
3) 0.529 - 0.538	5.4	30093.0	18831.3	38698.6
4) 0.538 - 0.547	5.7	30266.4	18964.2	38711.7
5) 0.547- 0.635	6.1	30530.2	20480.8	38480.1

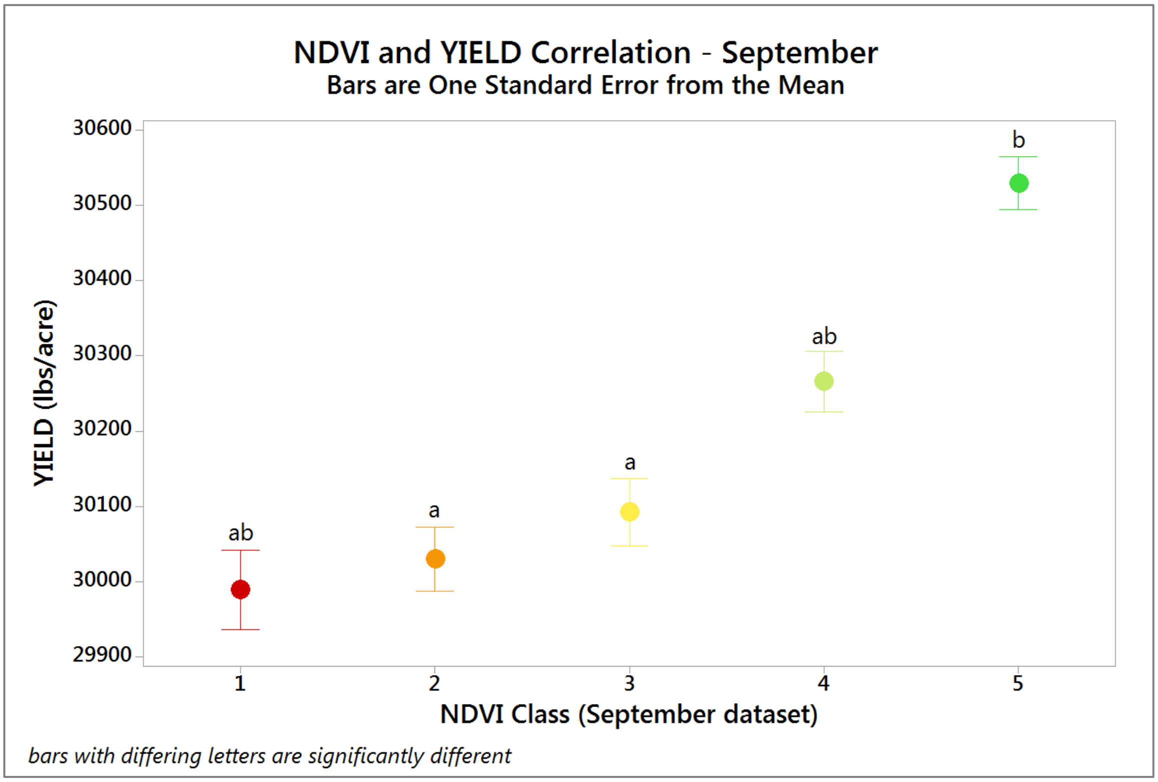

Figure 30: NDVI and Yield Correlation for September

Binning analysis for September indicates a positive correlation between NDVI and Yield. As NDVI values increase so too does yield. The difference between the mean yield for the highest and lowest NDVI class is approximately 540 lbs/acre.

3.6 Pixel by Pixel Analysis results

The following table and graphs show an example of the NDVI/Yield table containing 30,000 points as well as scatter plots for each of the datasets.

POINTID	YIELD	NDVI
1	26949.1	0.179
2	27350.2	0.242
3	28475.7	0.371
4	30053.8	0.264
5	29990.2	0.255
6	30030.0	0.214
7	30891.6	0.227
8	30101.0	0.228
9	29045.2	0.224
10	29048.4	0.203
11	29885.6	0.280
12	30652.0	0.365
13	31076.1	0.322
14	31625.8	0.273
15	31933.5	0.283
16	32639.1	0.490
17	32630.7	0.453
18	32623.5	0.405
19	32722.8	0.227
20	33159.4	0.293
21	34397.3	0.236
22	35045.7	0.290
23	26896.7	0.165
24	26937.8	0.252

Figure 31: Yield vs NDVI table sample after spatial join

This table shows the results of the Spatial Join in ArcGIS and contains a Yield value (lbs/acre), and an NDVI value for each 2m x 2m cell across the field for a total of approximately 30,000 records.

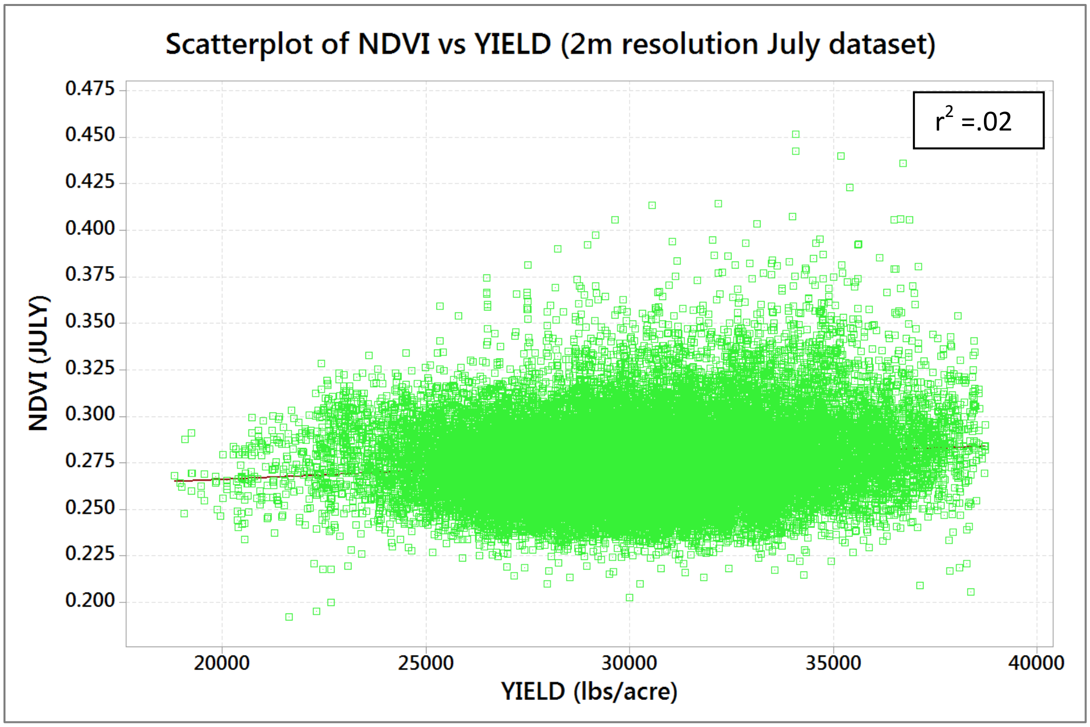

Figure32: NDVI vs Yield scatter plot for July (2m resolution)

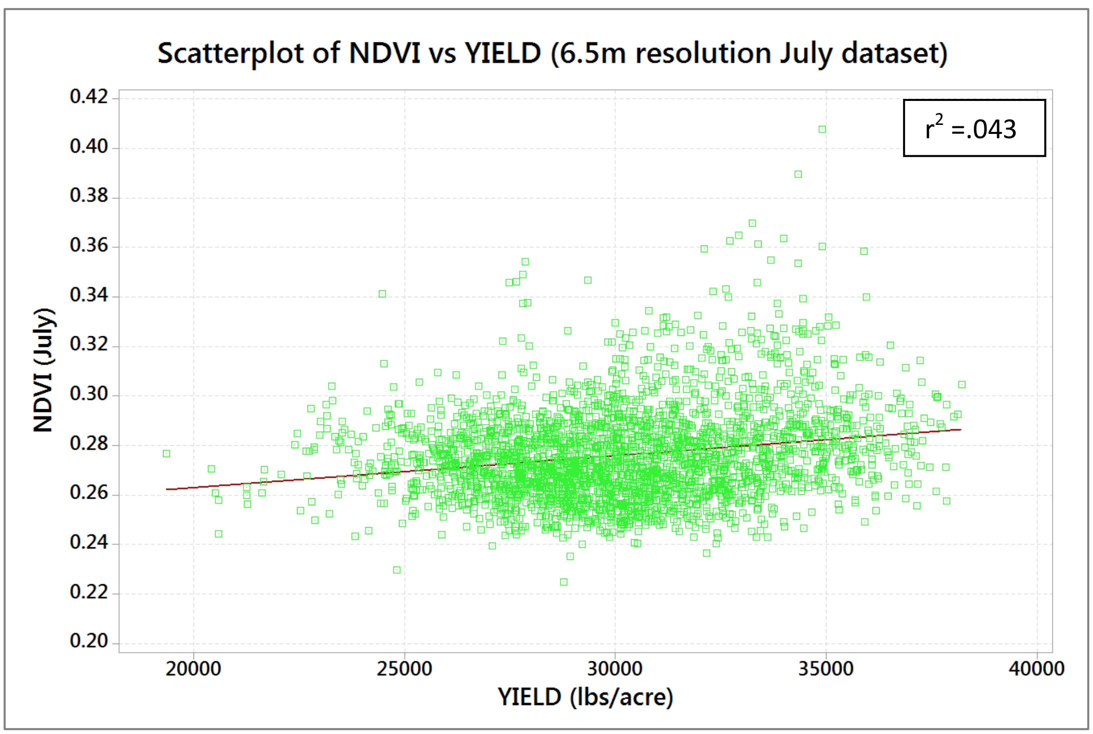

Figure 33: NDVI vs Yield scatter plot for July (6.5m resolution)

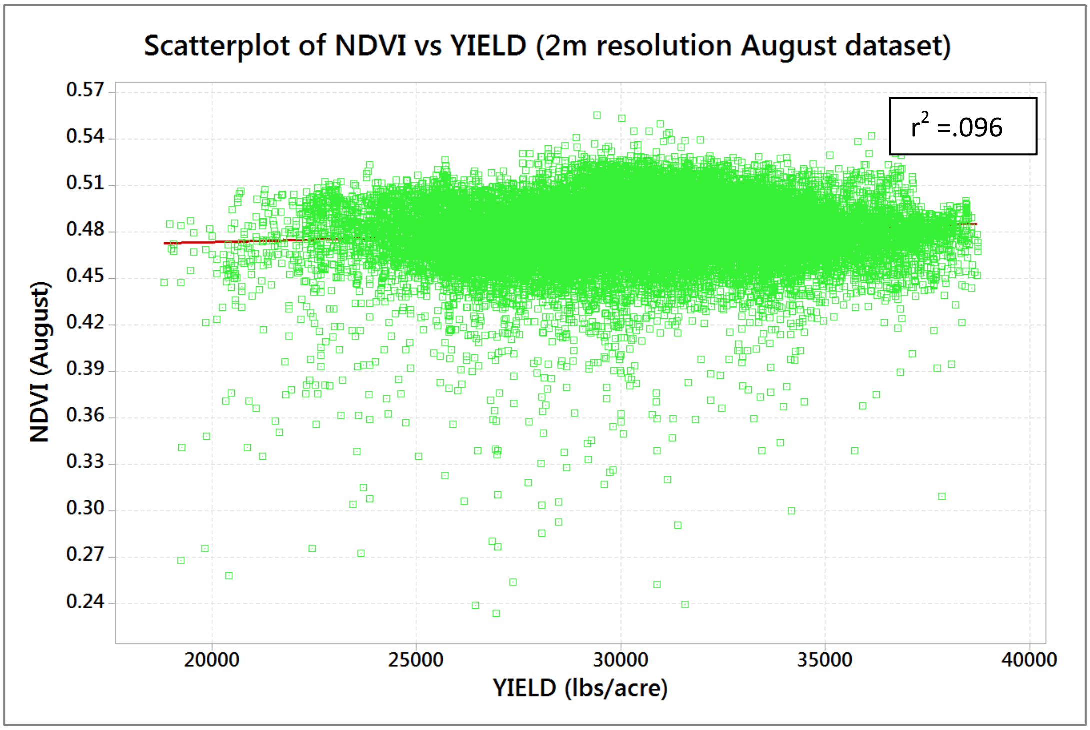

Figure 34: NDVI vs Yield scatter plot for August (2m resolution)

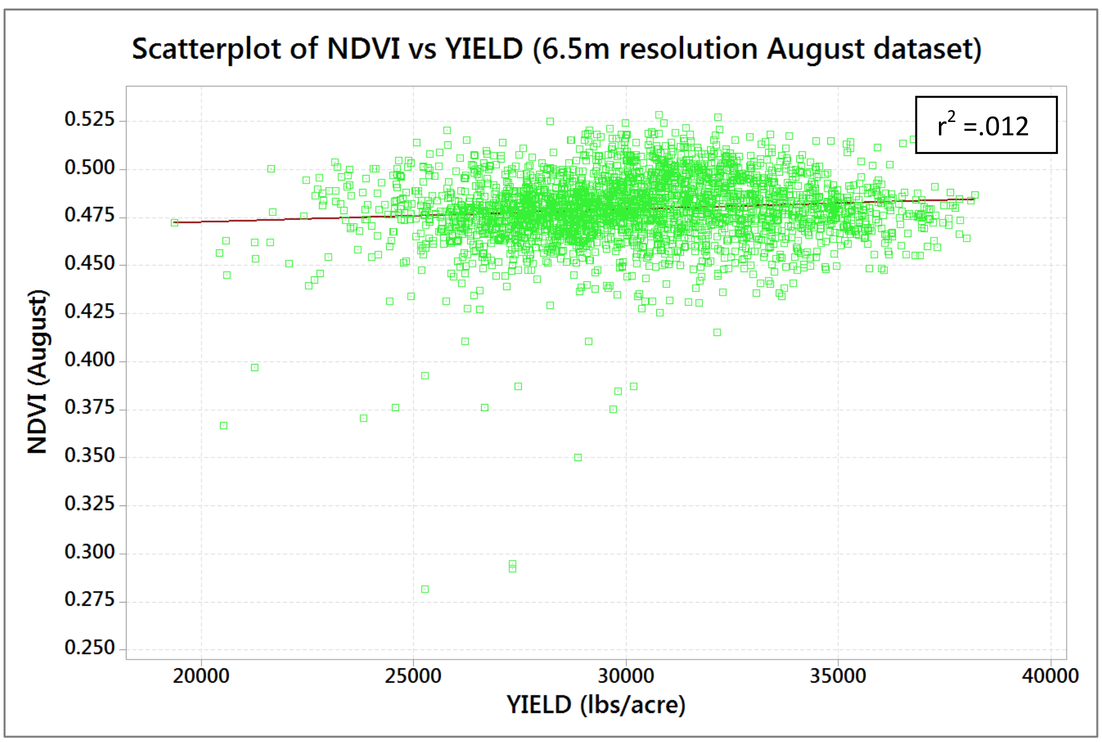

Figure 35: NDVI vs Yield scatter plot for August (6.5m resolution)

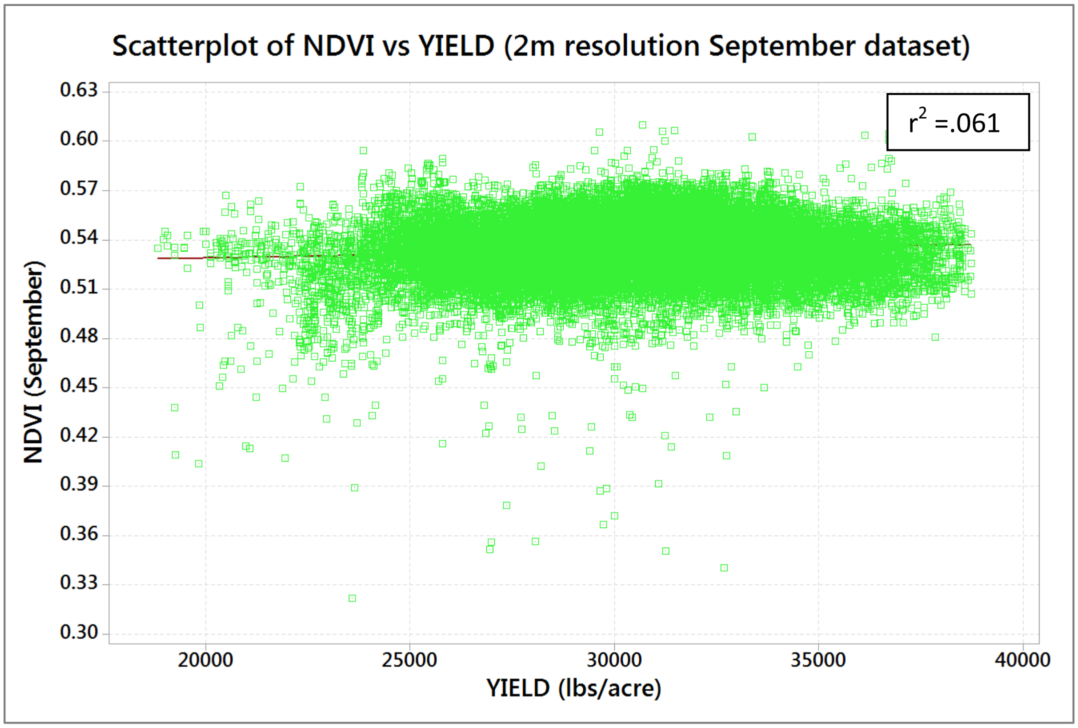

Figure 36: NDVI vs Yield scatter plot for September (2m resolution)

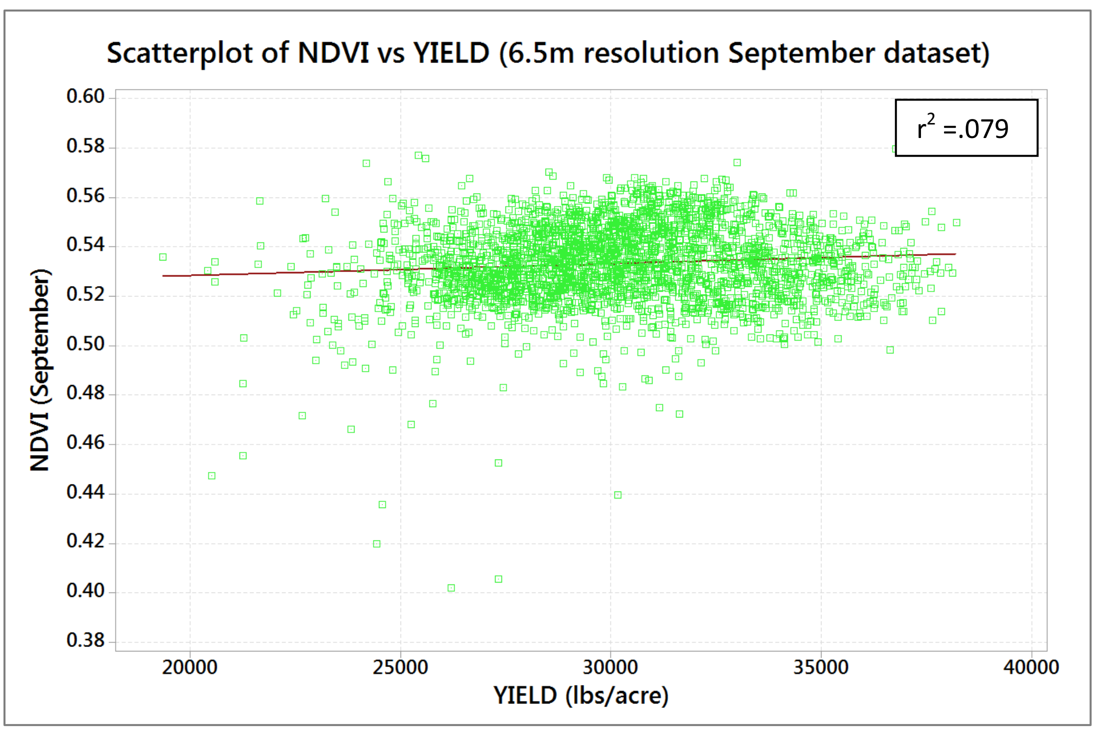

Figure 37: NDVI vs Yield scatter plot for September (6.5m resolution)

3.7 Multivariate Analysis

Multivariate Analysis Results (probabilities and RSq)					
Dataset (month)	**Resolution**	**Elevation**	**NDVI**	**4R**	**RSq**
July	*2m*	< 0.0001	< 0.0001	< 0.0001	0.0298
	6.5m	0.027	< 0.0001	< 0.0001	0.0548
August	*2m*	0.762	< 0.0001	< 0.0001	0.0346
	6.5m	0.732	< 0.0001	< 0.0001	0.0467
September	*2m*	< 0.0001	< 0.0001	< 0.0001	0.0218
	6.5m	0.0004	< 0.0001	< 0.0001	0.0318

Figure 38: Multivariate analysis results

Chapter 4: Discussion

4.1 Analyzing the Results

The binning analysis shows a strong correlation between NDVI and Yield for the July 13th (Growth Stage II – vegetative growth) and August 10th (Growth Stage IV – early bulking) datasets, while the correlation for the September 10th (Growth Stage IV – late bulking/early senescence) dataset is not as strong. These results are reasonable expectations since the crop begins to lose its vegetative vigour at later growth stages while leaves turn yellow and die off (Johnson, 2008).

The pixel by pixel analysis displayed relatively flat regression lines that trended upwards as NDVI and yield increased. Both July datasets (2m and 6.5m) returned the strongest correlations across all collection dates. Pixel by pixel analysis introduces much more variability in each dataset in comparison to the binning analysis. It is not surprising to see that the coarser resolution data (6.5m), resulted in stronger relationships between NDVI and yield in every dataset due to a decrease in variability by way of averaging more pixels across the field. The August and September datasets had mainly full canopy closure across the field, therefore NDVI values were averaging pixels that contained mostly vegetation while July NDVI values were averaging vegetation as well as bare soil due to the earlier growth stage of the crop. The difference in canopy size in July had an impact on the relationship between NDVI and yield in a positive way. Other ways to decrease variability in each dataset would be to incorporate other VIs such as Leaf Area Index, which have been used as a predictor of yield, and only take into account the amount of foliage cover (Harris, n.d.). Other studies have incorporated random yield samples throughout a field to compare with remotely sensed imagery. This would limit the amount of variation seen in the pixel by pixel analysis and would ensure that the yield value being used in the comparison was real and not an interpolated value (Al-Gaadi et al, 2016).

The multivariate analysis showed that three variables: Elevation, NDVI and Fertilizer treatment regime all had significant predictive ability for yield although RSq values were low. The July dataset, once again, provided the strongest correlation with yield out of the three collection dates. Coarser resolution data for all three months resulted in higher RSq values than higher resolution data due to decreased variability. I believe that the stronger correlation from the July model could be due to residual soil moisture leftover from the spring, which had an impact on crop growth and canopy size that ultimately led to higher NDVI values for those lower elevation areas where more moisture was present. The fertilizer treatment regime had little impact on NDVI or yield values. The next section includes additional discussion regarding elevation's impact on yield.

The stronger correlations between NDVI and Yield in three methods of analysis seen in the July 13th and August 10th datasets (crop age 39 days and 67 days respectively), indicates that capturing remotely sensed imagery between growth stage II and IV is best when attempting to predict yield in potatoes. This finding was also realized by Khalid A. Al-Gaadi et al. who observed that highest correlations between a VI from satellite imagery and yield was 60-70 days after planting in comparison with VI imagery from earlier and later crop growth stages (Al-Gaadi et al, 2016).

It is important to note that the goal of this study was not to attempt to predict actual quantity of potato yield in terms of lbs/acre for every pixel, but to identify broader areas of the target field that performed better or worse relative to the rest of the crop areas through the use of NDVI.

4.2 Topographic Features and Weather – Effects on Yield

The NDVI dataset that correlated greatest with Yield was from July 13th. The areas with highest NDVI values in that dataset were found in the Southern area of the field, which was also the lowest section in terms of elevation above sea level, as can be seen in the Digital Surface Model (figure 22). A study by Kumhalova, Jitka et al. observed that there was a strong correlation between topography and yield, specifically in drier years (Kumhalova et al, 2011). Climate data from the UPEI Climate Lab showed that station AC1 in Baltic, PE, located 6.5 km Northeast of the project study site, had a very dry month of July recording only 27.5mm of precipitation, approximately one third of the normal rainfall for the month of July for that area (Jardine, 2016). Climate data for August showed that there was less than average rainfall again with 76.9 mm (normal for August is 92.7mm) (Jardine, 2016). The farmer who manages the study site field acknowledged that this was a "very dry" summer and also observed that lower areas of the field seemed to produce the greatest at harvest.

The following map breaks down the field into five areas based on elevation (see figure 22 for reference). This map shows that the lowest and flattest area of the field (labeled "1" on the map), produced approximately 1,250 lbs/acre more than average.

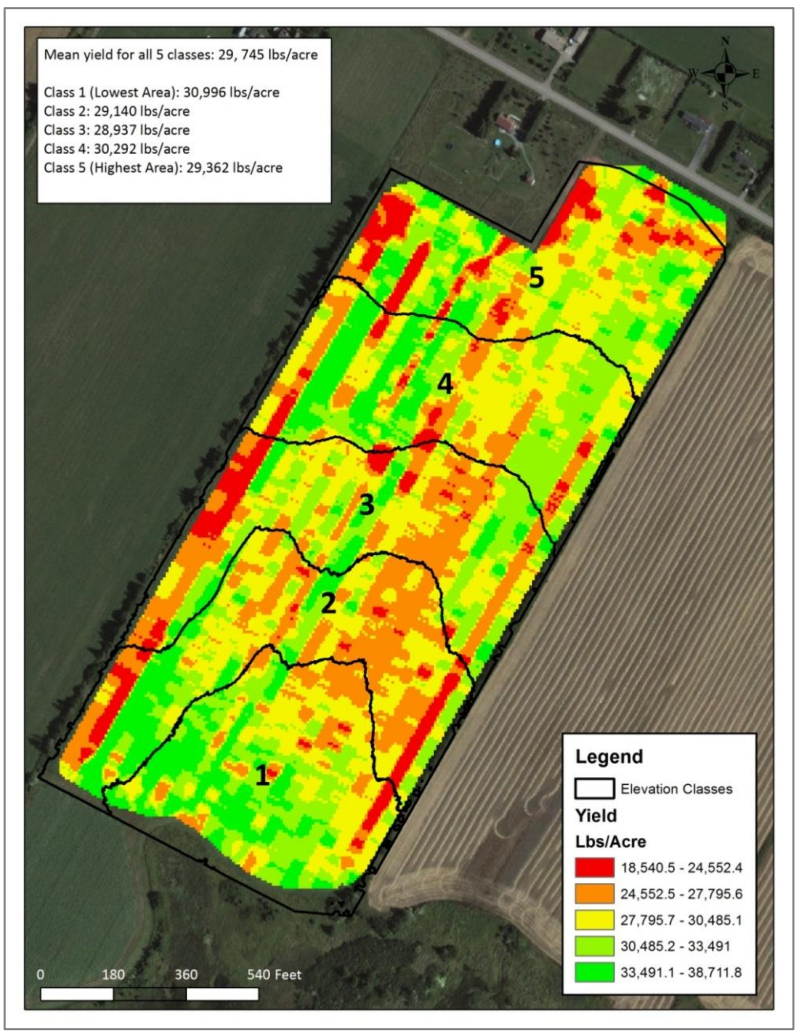

Figure 39: Map displaying 5 classes of elevation along with yield data

There are many other factors that affect yields of field crops, such as soil temperature and health characteristics, but topography (slope and aspect) and soil moisture - specifically in a dry summer, play a more significant role in determining production.

4.3 Using Vegetation Index Classes as Management Zones

One way to utilize the output vegetation index classes from a sUAS survey is to develop management zones (MZ). GIS and GPS play a key role, as the output classes can be accurately referenced to a place on the ground so that they can be combined with other important data layers such as soil health, topography, electrical conductivity, and past yield data to create distinct zones in a field with each zone receiving different amounts of nutrient input. These zones can then be used as an input file in a tractor with variable rate application capability and the farmer can let the system takeover while it applies appropriate rates of nutrients where they are needed. Nutrient application is not always reduced with the MZ approach versus uniform input application, but production can be increased since certain areas of a field do not require high amounts of input, and this excess can be redistributed to the areas which require more.

Identifying yield variation in crops is one of the first steps towards improving production. The difference between mean yield for the lowest and highest class of NDVI for the July dataset was 1,160 lbs/acre. The average price of potatoes in 2011 in P.E.I.

was 11.72 dollars per hundred weight (approximately 12c per lb) (P.E.I., 2016). This equates to a difference of approximately $139/acre in production between the lowest and highest classes of NDVI. Average farm size for P.E.I. in 2016 was 425 acres (StatsCan, 2017). A $139 difference per acre between the lowest and highest classes of NDVI on the average P.E.I. farm equates to $59,075. Eliminating yield variation altogether is not realistic since there are many factors involved, but improving production in the lower classes, and reducing inputs in the higher classes, or conversely - limiting inputs in consistently poor yielding areas and optimizing maximum yield potential areas is possible through PA management practices, and has the potential to positively effect a farmers' income.

A study by Hunt and Daughtry in 2017 assessed the use of sUAS as a tool in agriculture and summarized surveys of farmers in the U.S. from 2010 and 2012 and found that "about 50% of farmers track yields spatially in a field with yield monitors, but only about 20% spread fertilizer using variable rate applicators" (Hunt and Daughtry, 2017). These numbers would be largely influenced by wheat producers in the U.S., a sector of the agriculture industry where PA has seen more widespread adoption than in crops such as potatoes. These figures indicate that the full potential of sUAS in agriculture may not be realized until farmers make investments in other PA technologies such as variable rate applicators.

4.4 Recommendations for Further Studies

Further studies should include the use of a more capable multispectral camera that is able to capture additional bands of light besides RGB and NIR. The additional bands of light would allow further investigation into many vegetation indices – that could potentially represent a stronger relationship with yield in potatoes. Recently released multispectral cameras for use with sUAS, such as the Parrot Sequoia, come with sensors that record the amount of sunlight being collected by each band. This allows for radiometric calibration of the imagery and more accurate data (Parrot, 2016). In addition to collection of yield data by a monitor mounted to the harvester, other methods of yield data collection could be performed, such as digging manual samples at several random locations throughout the field. This would give an idea of absolute yield at those locations, and eliminate the need to use interpolation to estimate yield in areas between rows of points. It would also eliminate any possible issues with yield monitor or tractor operator error.

Studying multiple fields over a longer period of time would provide valuable information to understand the relationships between vegetation indices derived from sUAS captured imagery and yield. Following a potato crop through an entire rotation and comparing VIs with yield in rotational crops such as barley, soybeans, fall rye, winter wheat, etc. would provide information that could be compared between crops from one season to the next, and indicate the impact that variables such as topography, weather, soil moisture, or soil health have on yield.

4.5 Conclusions

This paper described the steps involved in using sUAS technology including planning and carrying out a mission, processing data, manipulating data in a GIS, and analyzing data in GIS and statistical software packages. The goal of this project was to determine whether in season vegetation index maps derived from sUAS collected imagery were an accurate predictor of yield in potatoes. It was determined that the areas which appeared healthiest early in the growing season (Growth stages II to early IV) tend to correlate well with measured yield at harvest when looking at broad “zones” within a field. The correlation at the single pixel level does not display as strong a relationship between NDVI and yield.

Satellite imagery still continues to be a viable option for gathering multispectral imagery of agricultural crops, especially over large areas. Multispectral satellite imagery as a yield prediction tool in potatoes has been successful in several studies, including those by Khalid A. Al-Ghaadi et al. (2016), and Johnson (2016). One of the main benefits of sUAS vs Satellite imagery is spatial resolution. For applications such as relative field health mapping and identification of yield variation, 1m to 2m resolution is sufficient. Limitations of satellite imagery are the potential presence of cloud cover and not having the flexibility to capture imagery at specific times as desired by the farmer or crop consultant. High resolution imagery from sUAS will be more important in applications such as disease, pest and weed detection.

SUAS will play a role as a remote sensing tool in agriculture for years to come. Paired with multispectral cameras and flown between potato growth stages II and IV, sUAS can be used to identify yield variations and help farmers and agronomists develop in-season management strategies to address issues and potentially improve production.

Farmers' uptake of sUAS technology will be slower than other more tangible technologies such as GPS. With GPS implemented for practices such as Auto-Steer, farmers see increased efficiency, and immediate results - which equals value. They are willing to spend over $40,000 on equipment that will pay for itself quickly by allowing them to operate equipment at night, ensuring straight rows and maximizing field cropping area, or enabling them to focus on certain implements while the tractor is guided by satellite navigation. sUAS have limitations from factors such as weather - wind and rain can suspend or prevent operations. When the wind is light during days in July and August, a farmer is likely too busy spraying crops to have time to fly sUAS over their fields and then process the data into actionable information in order to make a time sensitive management decision.

sUAS and data processing technology are advancing at such a rapid pace that certain methods and equipment used in this study could be considered "out of date" in the near future. To reproduce the methods used in this study, particularly in the data processing and analysis sections, would require at least an intermediate level of GIS knowledge and expertise. However, capturing and processing multispectral data for agriculture are becoming easier and more affordable. There are several online data processing platforms available where users can upload imagery and receive analysis, reports, maps and fertilizer recommendations back within 24 hours. These monthly fee subscriptions will be particularly attractive to farmers who cannot afford to spend time processing imagery, and do not have the means to purchase or operate expensive processing software. Crop consultants and agronomists would benefit from becoming trained in sUAS operations as well as processing spatial information and adding this service to their toolkit.

The yield monitor is an under-utilized tool and provides extremely valuable information that can be used as a report card for farmers' fields. At a price of approximately $10,000 this tool is affordable in comparison to some of the other on farm expenses paid every year (Greentronics, 2017). These tools may tell a farmer which areas of a field consistently yield less than others, and this information can be used to determine whether it is worth planting an expensive crop in lower producing areas of a field, or whether that area of the field would be better left out of production altogether. If the average cost per acre to grow potatoes is $3,000 per acre, then a farmer must yield at least 25,000 lbs per acre at 12c/lb to break even (Trainor, 2009; P.E.I., 2016). Once again, one of the limitations keeping farmers from adopting yield monitoring technology is dealing with data in a timely fashion.

There needs to be more collaboration between GIS and mapping professionals and those who work in agriculture such as farmers and agronomists. Each side has much to offer the other, and not only would the two sides involved benefit greatly from building relationships and cross-learning, but society as whole can gain from the growth and advancement of precision agriculture.

References

Adão, T., Hruška, J., Pádua, L., Bessa, J., Peres, E., Morais, R., & Sousa, J. (2017). Hyperspectral Imaging: A Review on UAV-Based Sensors, Data Processing and Applications for Agriculture and Forestry. Remote *Sensing, 9*(11), 1110. doi:10.3390/rs9111110

Agüera, F., Carvajal, F., & Pérez, M. (2012). Measuring Sunflower Nitrogen Status From An Unmanned Aerial Vehicle-Based System And An On The Ground Device. *Int. Arch. Photogramm. Remote Sens. Spatial Inf. Sci. ISPRS - International Archives of the Photogrammetry, Remote Sensing and Spatial Information Sciences, XXXVIII-1/C22*, 33-37. Retrieved March 10, 2016.

Al-Gaadi KA, Hassaballa AA, Tola E, Kayad AG, Madugundu R, Alblewi B, et al. (2016) Prediction of Potato Crop Yield Using Precision Agriculture Techniques. PLoS ONE 11(9): e0162219. https://doi.org/10.1371/journal.pone.0162219

Anthony, D., Elbaum, S., Lorenz, A., & Detweiler, C. (2014). On crop height estimation with UAVs. *2014 IEEE/RSJ International Conference on Intelligent Robots and Systems*. doi:10.1109/iros.2014.6943245

AUVSI. (2013). The Economic Impact of Unmanned Aircraft Systems Integration in the United States. Retrieved April, 2016, from https://higherlogicdownload.s3.amazonaws.com/AUVSI/958c920a-7f9b-4ad2-9807-f9a4e95d1ef1/UploadedImages/New_Economic Report 2013 Full.pdf

Bala, S. K., & Islam, A. S. (2009). Correlation between potato yield and MODIS-derived vegetation indices. *International Journal of Remote Sensing, 30*(10), 2491-2507. doi:10.1080/01431160802552744

Bendig, J., Bolten, A., Bennertz, S., Broscheit, J., Eichfuss, S., & Bareth, G. (2014). Estimating Biomass of Barley Using Crop Surface Models (CSMs) Derived from UAV-Based RGB Imaging. *Remote Sensing, 6*(11), 10395-10412. Retrieved February 5, 2016.

Cambouris, A. N., Zebarth, B. J., Ziadi, N., & Perron, I. (2014). Precision Agriculture in Potato Production. Potato Res. Potato Research, 57(3-4), 249-262. Retrieved March 21, 2016.

Canadian Cancer Society's Advisory Committee on Cancer Statistics. Canadian Cancer Statistics 2013. Toronto, ON: Canadian Cancer Society; 2013.

Colwell R. (1956). Determining the prevalence of certain cereal crop diseases by means of aerial photography. *Hilgardia 26*(5):223-286. DOI:10.3733/hilg.v26n05p223

Cunha, M., Marçal, A. R., & Silva, L. (2010). Very early prediction of wine yield based on satellite data from VEGETATION*. International Journal of Remote Sensing, 31*(12), 3125-3142. doi:10.1080/01431160903154382

Digital Globe Products & Services. (n.d.). Retrieved February 02, 2018, from https://www.digitalglobe.com/resources/satellite-information

DJI Matrice 100: The quadcopter for developers - DJI. (n.d.). Retrieved February 02, 2018, from https://www.dji.com/matrice100

DroneDeploy (2017). Seven Ways to Improve the Accuracy of Your Drone Maps. Retrieved May 1, 2017, from https://blog.dronedeploy.com/seven-ways-to-improve-the-accuracy-of-your-drone-maps-9d3161f05956

ESRI. (n.d.). Data classification methods. Retrieved May 12, 2017, from http://pro.arcgis.com/en/pro-app/help/mapping/symbols-and-styles/data-classification-methods.htm#ESRI_SECTION1_1BDD383C17164B948BF546CEADDA70E9

ESRI. (n.d.). How Kriging works. Retrieved June 10, 2017, from http://desktop.arcgis.com/en/arcmap/10.3/tools/3d-analyst-toolbox/how-kriging-works.htm

Evert, F. K., Booij, R., Jukema, J. N., Berge, H. F., Uenk, D., Meurs, E. (., . . . Slabbekoorn, J. (. (2012). Using crop reflectance to determine sidedress N rate in potato saves N and maintains yield. *European Journal of Agronomy, 43*, 58-67. Retrieved March 12, 2016.

Ferencz, Csaba & Bognár, P & Lichtenberger, János & Hamar, Daniel & Tarcsai, Gy & Timár, Gábor & Molnár, Gábor & Pásztor, Szilárd & Steinbach, Peter & Székely, Balázs & E Ferencz, Orsolya & Ferencz-Árkos, I. (2004). Crop yield estimation by satellite remote sensing. *International Journal of Remote Sensing. 25*. 4113-4149. 10.1080/01431160410001698870.

Fertilizer Canada (2017). Nutrient Stewardship. Retrieved February 15, 2018, from https://fertilizercanada.ca/nutrient-stewardship/.

Frost, J. (2013). Regression Analysis: How Do I Interpret R-squared and Assess the Goodness-of-Fit? Retrieved September 27, 2017, from http://blog.minitab.com/blog/adventures-in-statistics-2/regression-analysis-how-do-i-interpret-r-squared-and-assess-the-goodness-of-fit

Gebbers, R., & Adamchuk, V. I. (2010). Precision Agriculture and Food Security. *Science, 327*(5967), 828-831. doi:10.1126/science.1183899. Retrieved January 29, 2018.

Geipel, J., Link, J., Wirwahn, J., & Claupein, W. (2016). A Programmable Aerial Multispectral Camera System for In-Season Crop Biomass and Nitrogen Content Estimation. *Agriculture, 6(1),* 4. Retrieved March 15, 2016.

Gómez-Candón, D., Castro, A. I., & López-Granados, F. (2013). Assessing the accuracy of mosaics from unmanned aerial vehicle (UAV) imagery for precision agriculture purposes in wheat. *Precision Agric Precision Agriculture, 15*(1), 44-56. Retrieved January 28, 2016.

GreenTronics. (2017). RiteYield – Yield Monitor. Retrieved July 10, 2017, from http://greentronics.com/products/yield-monitor/

Harris Geospatial. (n.d.). Broadband Greenness. Retrieved May 10, 2016, from https://www.harrisgeospatial.com/docs/BroadbandGreenness.html

Hiniker (2015). Hiniker granular stainless steel side-dress applicator. Retrieved September 20, 2017, from http://www.agprofessional.com/news/products/hiniker-granular-stainless-steel-side-dress-applicator

Hunt, E. R., & Daughtry, C. S. (2017). What good are unmanned aircraft systems for agricultural remote sensing and precision agriculture? *International Journal of Remote Sensing*, 1-32. doi:10.1080/01431161.2017.1410300

Jardine, D. (2016). *UPEI Climate Research Lab Monthly Meteorological Summary - July, 2016* (Rep.). UPEI Climate Research Lab.

Jardine, D. (2016). *UPEI Climate Research Lab Monthly Meteorological Summary – August, 2016* (Rep.). UPEI Climate Research Lab.

Johnson, D. A., ed., (2008), Potato Health Management, 2nd ed., American Phytopathological Society, St. Paul, MN.

Johnson, D. M. (2016). A comprehensive assessment of the correlations between field crop yields and commonly used MODIS products. *International Journal of Applied Earth Observation and Geoinformation, 52*, 65-81. doi:10.1016/j.jag.2016.05.010

Kumhálová, J., Kumhála, F., Kroulík, M., & Matějková, Š. (2011). The impact of topography on soil properties and yield and the effects of weather conditions. *Precision Agriculture*, 12(6), 813-830. doi:10.1007/s11119-011-9221-x

MacDonald, M. (2012). Potatoes: A billion dollar industry for P.E.I. Retrieved May 06, 2017, from http://www.theguardian.pe.ca/news/local/2012/2/26/potatoes-a-billion-dollar-industry-for-2907927.html

Macdonald, M. (2013). Pesticide runoff suspected in latest case of dead fish in PEI river. Retrieved March 06, 2017, from https://beta.theglobeandmail.com/news/national/pesticide-runoff-suspected-in-latest-case-of-dead-fish-in-peiriver/article13481109/?ref=http://www.theglobeandmail.com&

Matese, A., Toscano, P., Gennaro, S. D., Genesio, L., Vaccari, F., Primicerio, J., . . . Gioli, B. (2015). Intercomparison of UAV, Aircraft and Satellite Remote Sensing Platforms for Precision Viticulture. *Remote Sensing, 7*(3), 2971-2990. doi:10.3390/rs70302971

Mulla, D. J. (2013). Twenty five years of remote sensing in precision agriculture: Key advances and remaining knowledge gaps. *Biosystems Engineering, 114*(4), 358-371. Retrieved March 20, 2016.

Micro Hyperspec. (n.d.). Retrieved April 06, 2016, from http://www.headwallphotonics.com/spectral-imaging/hyperspectral/micro-hyperspec

Miller, K. (2016). Is your Yield set by Mid-June? A Correlation Analysis Between NDVI and Yield. Retrieved March 20, 2016, from https://www.linkedin.com/pulse/your-crop-yield-set-july-correlation-between-ndvi-map-kyle-miller

Mittelstaedt, M. (2006). 'Pesticides are what is killing our kids'. Retrieved May 01, 2017, from https://beta.theglobeandmail.com/news/national/pesticides-are-what-is-killing-ourkids/article18179217/?ref=http%3A%2F%2Fwww.theglobeandmail.com&page=all

National Research Council. *Precision Agriculture in the 21st Century*; National Academy Press: Washington, DC,USA,1997; p. 149.

NDVI Camera – NGB Converted Canon S110 Camera. (n.d.). Retrieved June 01, 2017, from https://event38.com/product/ndvi-camera-ngb-converted-canon-s110-camera/

Nigon, T. J., Mulla, D. J., Rosen, C. J., Cohen, Y., Alchanatis, V., Knight, J., & Rud, R. (2015). Hyperspectral aerial imagery for detecting nitrogen stress in two potato cultivars. *Computers and Electronics in Agriculture, 112,* 36-46. Retrieved March 12, 2016.

Parrot. (2016). *Parrot Sequoia Technical Specifications* [Brochure]. Retrieved May 12, 2017, from https://www.sensefly.com/fileadmin/user_upload/sensefly/documents/brochures/Sequoia_Specifications_2016_sensefly.pdf/

P.E.I. Department of Agriculture and Fisheries. (2016) 2016 Agriculture Statistical Report (Rep.). P.E.I. Department of Agriculture and Fisheries. https://www.princeedwardisland.ca/sites/default/files/publications/af_stat_all2016.pdf

P.E.I. Department of Communities, Lands and Environment, Resource Inventory, 2010, Corporate Land Use Inventory 2010

Pix4D. (n.d.). Selecting the Image Acquisition Plan Type. Retrieved May 12, 2017, from https://support.pix4d.com/hc/en-us/articles/202557459-Step-1-Before-Starting-a-Project-1-Designing-the-Image-Acquisition-Plan-a-Selecting-the-Image-Acquisition-Plan-Type#gsc.tab=0

Photogrammetry. (n.d.). Retrieved June 06, 2017, from http://www.remoteaerialsurveys.co.uk/photogrammetry

Prince Edward Island has the largest potato crop in Canada (Rep. No. 95-640-X). (2017, May 10). Retrieved June 1, 2017, from Statistics Canada website: http://www.statcan.gc.ca/pub/95-640-x/2016001/article/14801-eng.pdf

Oliver, M. A., & Webster, R. (2015). *Basic steps in geostatistics: the variogram and kriging*. Cham, Switzerland: Springer.

Rasmussen, J., Ntakos, G., Nielsen, J., Svensgaard, J., Poulsen, R. N., & Christensen, S. (2016). Are vegetation indices derived from consumer-grade cameras mounted on UAVs sufficiently reliable for assessing experimental plots? *European Journal of Agronomy, 74*, 75-92. Retrieved January 28, 2016.

Rey-Caramés, C., Diago, M., Martín, M., Lobo, A., & Tardaguila, J. (2015). Using RPAS Multi-Spectral Imagery to Characterise Vigour, Leaf Development, Yield Components and Berry Composition Variability within a Vineyard. *Remote Sensing, 7*(12), 14458-14481. doi:10.3390/rs71114458

Transport Canada (2018). Flying *your drone safely and legally - Transport Canada*. Retrieved January 29, 2018 from: https://www.tc.gc.ca/eng/civilaviation/opssvs/flying-drone-safely-legally.html

Torres-Sánchez, J., Peña, J., Castro, A. D., & López-Granados, F. (2014). Multi-temporal mapping of the vegetation fraction in early-season wheat fields using images from UAV. *Computers and Electronics in Agriculture, 103*, 104-113. doi:10.1016/j.compag.2014.02.009

Trainor, P. J. (2009). Bucks in the ground: the cost to grow an acre of potatoes. *Prince Edward Island Potato News,* 10(3). Retrieved December 20, 2016.

United Nations, Department of Economic and Social Affairs, Population Division (2015). *World Population Prospects: The 2015 Revision, Key Findings and Advance Tables*. Working Paper No. ESA/P/WP.241.

Westoby, M., Brasington, J., Glasser, N., Hambrey, M., & Reynolds, J. (2012). 'Structure-from-Motion' photogrammetry: A low-cost, effective tool for geoscience applications. *Geomorphology, 179*, 300-314. doi:10.1016/j.geomorph.2012.08.021

Yang, C., Everitt, J. H., & Bradford, J. M. (2006). Evaluating High-Resolution QuickBird Satellite Imagery for Estimating Cotton Yield. *Transactions of the ASABE (American Society of Agricultural and Biological Engineers)*, 49(5), 1599-1606. doi:10.13031/2013.22034

Yu, Z., Cao, Z., Wu, X., Bai, X., Qin, Y., Zhuo, W., . . . Xue, H. (2013). Automatic image-based detection technology for two critical growth stages of maize: Emergence and three-leaf stage. *Agricultural and Forest Meteorology, 174-175*, 65-84. doi:10.1016/j.agrformet.2013.02.011

Zaman-Allah, M., Vergara, O., Araus, J. L., Tarekegne, A., Magorokosho, C., Zarco-Tejada, P. J., .Cairns, J. (2015). Unmanned aerial platform-based multi-spectral imaging for field phenotyping of maize. *Plant Methods, 11*(1). Retrieved March 10, 2016.

Zhang, C., & Kovacs, J. M. (2012). The application of small unmanned aerial systems for precision agriculture: a review. *Precision Agriculture, 13*(6), 693-712. doi:10.1007/s11119-012-9274-5

Zhang, N., Wang, M. and Wang, N. (2002), 'Precision agriculture-a worldwide overview', *Computers and Electronics in Agriculture*, vol. 36(2), 113 – 132.

Zhang, Q. (2016). *Precision Agriculture Technology for Crop Farming*. Boca Raton, FL: Taylor and Francis Group.

Appendix

Table 3 – Other PEI Climate Recording Stations – July, 2016

	Map ID	Tmean C	Tmax C	Tmin C	Total Ppt mm	Total Snow Cm	Max Wind Gust (km/h)	Avg. Wind Speed km/h	# of Frost Days <=0°C
East Pt	EC9	17.7	27.4	10.7	42.0	0	54.0	16.9	0
St. Peters	EC8	18.6	29.5	9.1	52.4	0	56.0	12.3	0
Peters Rd	EC7	19.9	29.5	9.5	76.6	0			0
Harrington	AC2	18.9	28.8	10.1	39.4	0	59.0	10.9	0
Ch'town A	EC6	18.9	28.1	8.9	72.0	0	56.0		0
Elmwood	EC5	18.8	28.8	9.1	81.5	0	33.8	5.8	0
New Glasgow	EC3	19.0	28.5	7.5	45.0	0			0
Maple Plains	EC4	18.1	29.9	5.4	46.0	0	28.5	9.1	0
Summerside A	EC2	18.6	28.9	8.1	60.3	0	82.0	15.0	0
North Cape	EC1	16.7	29.7	5.0	66.6	0	91.0	18.2	0
Baltic (Prince Co.)	AC1	18.9	29.3	8.9	27.5	0	38.6	11.2	0

- ***Missing data***

Figure A1: Table displaying Climate station data for July 2016
Source: UPEI Climate Research Lab

Table 7 – Variation ofJuly2016 Total Precipitation Amounts from 1981-2010 Climate Normal

Climate Station	Total PPT in mm July 2016	30 Year Normal C 1981-2010	Variation from Normal mm
East Point - EC	42.0	86.6	-44.60
Dingwells	56.9	79.3	-22.40
St. Peters	52.4	79.3	-26.90
Cardigan Head	30.0	79.3	-49.30
Flat River	66.5	79.9	*-13.40*
Orwell	48.5	79.9	*-31.40*
Peters Rd/Alliston	76.6	79.9	*-3.30*
Alliston CNP	64.8	79.9	*-15.10*
Harrington	39.4	79.9	*-40.50*
Charlottetown A	72.0	79.9	-7.90
Winsloe South	56.4	79.9	-23.50
Elmwood	81.5	87.5	-6.00
St. Catherine's	62.0	79.9	-17.90
Borden - Carleton	64.2	74.4	-10.20
Summerside A	60.3	74.1	-13.80
Baltic	27.5	74.1	-46.60
Foxley River	64.3	96.0	-31.70
North Cape	66.6	79.7	-13.10
Cape Egmont	26.7	74.1	Cal
Brockton	29.5	79.7	-50.20
Hampton	72.6	74.1	-1.50
Glen Valley	19.6	78.6	Cal
Fanning Brook	50.3	79.9	-29.60
Arlington	44.0	96.0	-52.00
East Point – UP16	57.0	86.6	-29.60
New Glasgow	45.0	78.6	-33.60
White Sands	51.8	79.9	-28.10
Tignish	47.8	79.7	-31.90
Maple Plains	46.0	74.1	-28.10

*- Data not complete due to technical issues or no heater on unit
M – Missing data
Cal – Rain gauge requires calibration

Figure A2: Table displaying July 2016 Precipitation Data vs 30 year normals
Source: UPEI Climate Research Lab

Table 3 – Other PEI Climate Recording Stations – August, 2016

	Map ID	Tmean C	Tmax C	Tmin C	Total Ppt mm	Total Snow Cm	Max Wind Gust (km/h)	Avg. Wind Speed km/h	# of Frost Days <=0°C
East Pt	EC9	18.4	26.1	11.8	61.5		72.0	18.6	0
St. Peters	EC8	18.9	28.6	10.0	74.9		56.0	13.7	0
Peters Rd	EC7	19.4	28.0	12.5	141.7				0
Harrington	AC2	18.7	27.8	10.6	134.8		59.0	12.6	0
Ch'town A	EC6	18.7	27.8	8.9	120.4		67.0		0
Elmwood	EC5	18.4	27.5	7.9	71.4		38.6	6.6	0
New Glasgow	EC3	18.5	27.5	7.5	113.8				0
Maple Plains	EC4	17.8	27.4	4.9	101.4		24.4	9.2	0
Summerside A	EC2	19.0	28.4	8.2	82.8		61.0	16.2	0
North Cape	EC1	17.5	28.3	7.5	85.3		65.0	21.2	0
Baltic (Prince Co.)	AC1	18.8	28.1	9.3	76.9		32.9	11.5	0

- ***Missing data***

Figure A3: Table displaying Climate station data for August 2016
Source: UPEI Climate Research Lab

Table 7 – Variation of August 2016 Total Precipitation Amounts from 1981-2010 Climate Normal

Climate Station	Total PPT in mm August 2016	30 Year Normal C 1981-2010	Variation from Normal mm
St. Peters	74.9	88.9	-14.00
Cardigan Head	25.6	88.9	M
Flat River	100.6	95.7	*4.90*
Orwell	92.7	95.7	*-3.00*
Peters Rd/Alliston	141.7	95.7	*46.00*
Alliston CNP	115.3	95.7	*19.60*
Harrington	134.8	95.7	*39.10*
Charlottetown A	120.4	95.7	24.70
Winsloe South	115.8	95.7	20.10
Elmwood	71.4	87.5	-16.10
St. Catherine's	76.2	95.7	-19.50
Borden - Carleton	106.6	92.7	13.90
Summerside A	82.8	92.7	-9.90
Baltic	76.9	92.7	-15.80
Foxley River	68.8	87.7	-18.90
North Cape	85.3	79.7	5.60
Cape Egmont	94.0	92.7	1.30
Brockton	59.4	79.7	-20.30
Hampton	82.4	92.7	-10.30
Glen Valley	84.8	87.5	-2.70
Fanning Brook	83.8	95.7	-11.90
Arlington	55.4	87.7	-32.30
East Point – UP16	78.2	103.6	-25.40
New Glasgow	113.8	87.5	26.30
White Sands	79.8	95.7	-15.90
Tignish	64.3	79.7	-15.40
Maple Plains	101.4	92.7	8.70

M – Missing data

Figure A4: Table displaying August 2016 Precipitation Data vs 30 year normals
Source: UPEI Climate Research Lab

Quality Report

Generated with Pro version 2.1.61

Important: Click on the different icons for:

Help to analyze the results in the Quality Report

Additional information about the sections

Click here for additional tips to analyze the Quality Report

Summary

Project	ramsayjul13ngb
Processed	2016-07-27 16:41:51
Average Ground Sampling Distance (GSD)	3.33 cm / 1.31 in
Area Covered	0.2363 km^2 / 23.6342 ha / 0.0913 sq. mi. / 58.4317 acres
Time for Initial Processing (without report)	30m:37s

Quality Check

Images	median of 26240 keypoints per image	
Dataset	236 out of 236 images calibrated (100%), all images enabled	
Camera Optimization	1.48% relative difference between initial and optimized internal camera parameters	
Matching	median of 12858.3 matches per calibrated image	
Georeferencing	yes, 4 GCPs (4 3D), mean RMS error = 0.015 m	

Preview

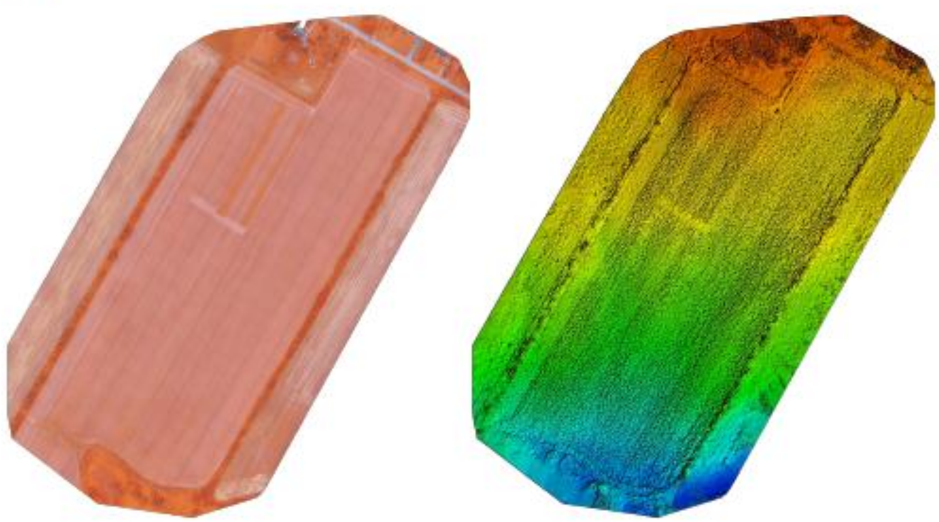

Figure 1: Orthomosaic and the corresponding sparse Digital Surface Model (DSM) before densification.

Figure A5: Pix4D Quality Report sample for July dataset

Figure A6: Near-Infrared Orthomosaic for July dataset

Figure A7: Near-Infrared Orthomosaic for August dataset

Figure A8: Near-Infrared Orthomosaic for September dataset

Figure A9: Original, Unfiltered Yield Data points clipped to study area